University of Genoa
Department of Neuroscience, Rehabilitation, Ophthalmology,
Genetics, and Maternal and Children's Sciences (DINOGMI)

-

In partial fulfillment of the requirements for the degree of

Doctor of Philosophy in Neuroscience

MICROSTRUCTURAL WHITE MATTER PROPERTIES IN MULTIPLE SCLEROSIS: ANATOMICAL SPATIAL MAPPING VIA NODDI MODELLING TO BETTER UNDERSTAND THE MECHANISM OF INJURY

Candidate	*Supervisors*	*Co-Supervisor*
Niccolo' Piaggio	**Luca Roccatagliata** **Matilde Inglese**	**Matteo Pardini**

to my supervisors LR and MP,

who heroically kept me "*on the tracks*" along all the railway to doctorate
and made me believe in it, winning my hesitations
until this final gratifying achievement.

to GB, GZ and CP,

the three essential inspiring figures who stayed at my side "*in their own way*"
along, respectively, the three parts of this long university journey:
school of medicine, internship of specialization and PhD course.

to my parents EA and MP

& all my historical friends GR, RP, LV, BC, VT, MF,
…the ones who (chosen or not) were *always* there to support me
from the beginning to the end of this great ascent.

to my brother BP,

who shared with me this inexplicable
interchangeable academic destiny.

…to *ALL* of you,

I dedicate this 3rd thesis,
that will –likely– be
the *last* thesis of my life.

Twenty years from now you will be more disappointed
by the things that you didn't do than by the ones you did do.
So throw off the bowlines.
Sail away from the safe harbor.
Catch the trade winds in your sails.
Explore.
Dream.
***Discover**.*

Mark Twain

We are going to fight.
We are going to be hurt.
*And, in **the end**, we will stand.*

Stephen King

SUMMARY

List of Abbreviations

AD	-	Axial Diffusivity
ADC	-	Apparent Diffusion Coefficient
BASH	-	Bourne Again SHell
BET	-	Brain Extraction Tool
BOLD	-	Blood Oxygen Level Dependent
CIS	-	Clinically Isolated Syndrome
CNS	-	Central Nervous System
CSF	-	Cerebro-Spinal Fluid
CST	-	Cortico-Spinal Tract
DIS	-	Dissemination In Space
DIT	-	Dissemination In Time
DKI	-	Diffusion Kurtosis Imaging
DSI	-	Diffusion Spectrum Imaging
DTI	-	Diffusion Tensor Imaging
DWI	-	Diffusion Weighted Imaging
EDSS	-	Expanded Disability Status Scale
F	-	Female
FA	-	Fractional Anisotropy
FAST	-	FSL Automated Segmentation Tool
FICVF	-	Intracellular Volume Fraction (= ND)
FISO	-	Free-Water Isotropic Volume Fraction (= ISO)
FLAIR	-	Fluid Attenuated Inversion Recovery
FLIRT	-	FSL Linear registration Tool
FSL	-	Functional MRI of the Brain Software Library

FWI	-	Free Water Imaging
GM	-	Gray Matter
GNU	-	General Public License
ISO	-	Isotropic Volume Fraction (= FISO)
M	-	Male
MATLAB	-	MATrix LABoratory
MD	-	Mean Diffusivity
MNI	-	Montreal Neurological Institute
MPRAGE	-	Magnetization-Prepared Rapid Acquisition Gradient Echo
MR	-	Magnetic Resonance
MRI	-	Magnetic Resonance Imaging
MS	-	Multiple Sclerosis
N	-	Number
ND	-	Neurite Density (= FICVF)
NODDI	-	Neurite Orientation, Dispersion and Density Imaging
ODI	-	Orientation Dispersion Index
PDI	-	Permeability-Diffusivity Imaging
PP	-	Primary Progressive
QTI	-	Q-Space Trajectory Imaging
RD	-	Radial Diffusivity
RR	-	Relapsing Remitting
SP	-	Secondary Progressive
STD	-	Standard Deviation
TE	-	Echo Time
TOT	-	Total
TR	-	Repetition Time
WM	-	White Matter

Acknowledgements

Besides the people to which this thesis is dedicated, several thanks are deserved by other people who contributed and supported the birth and development of this work.

Thanks to Professor Matilde Inglese, who opened for me the doors to neurosciences and guided me through the first steps of this windy road.

Thanks to the Professors Giovanni Luigi Mancardi, Mario Amore and Antonio Uccelli for offering me a way to build my research path in the department of Neurology, Rehabilitation, Ophthalmology, Genetics, Maternal and Child Health and to be part of the Sys4MS project team.

Thanks to the radiology staff of I.S.T. and G.Gaslini Hospitals, who kindly hosted our MRI acquisitions and welcomed our patients.

Thanks to my new radiology colleagues at D.I.T.: Agostino Taccone, Piero Glorialanza, Claudia Debenedetti, and especially Marco Estienne: without their frequent sacrifices I wouldn't have had any chance to finish this work within the maximum times.

Special thanks to all the people who made of "the LAB" the greatest place in which I ever worked: Giulia Bommarito, Simona Schiavi, Matteo Martino, Paola Magioncalda, Caterina Lapucci, Giacomo Boffa, Elvira Sbragia, Riccardo Iandolo, Benedetta Conio, Alessandro Bellini, Lorenzo Cama, Laura Falcitano, […] and all the others with which we shared a funny time … "wandering among the voxels".

1. Abstract

Introduction. Plenty of literature focused on the topography of multiple sclerosis (MS) injury localization within brain.
Various theories were proposed to explain this pattern, calling into question two main hypothesis:
1- preexistent tissue-intrinsic microstructural susceptibility factors
2- cerebrospinal-fluid (CSF)-borne soluble inflammatory factors diffusing through the brain surfaces (inner-ependymal-ventricular and outer-pial-cortical), thence affecting the parenchyma with a decreasing distribution along a distance-from-CSF gradient.
However, despite more than one hundred years of efforts, the etio-physio-pathological basis of the onset and development of the MS plaque has not been completely unveiled yet.
Recent technological advances in magnetic resonance imaging (MRI) and data post-processing, enabling an in-vivo definition of the local microstructure of the white matter (WM), give new perspectives for untangling the secrets of this complex disease.

Materials & Methods. With a novel algorithm to analyze diffusion weighted MRI images, "NODDI", we created detailed atlases of the microstructural characteristics of the normal WM in a healthy population; parallelly, we defined the topography of the lesions for a MS-affected population.
By superposition of the patients lesion maps onto the healthy atlas, we could then test if any of the microstructural NODDI parameters is predictive of development of a T1-visible lesion.
We then tested at which deepness of the gradient of distance from CSF, the a-priori microstructural susceptibility factor was more responsible of the T1-visible lesion development.
Finally, we computed the mean distance from the CSF of the T1-lesioned tissue, compared to the T1-spared one.

Results. In the corresponding areas where the patients developed T1-visible lesions, we found significant higher values of Neurite Density (ND) on the healthy population atlas, if compared to the areas where no lesion was visible on T1 imaging.
The a-priori tissue property of high ND was found to have its greatest influence on T1-visible lesion formation especially in the deep WM layer (the furthest from the pial and ventricular surfaces).
The NODDI microstructural parameter Orientation Dispersion Index (ODI) showed to have no influence at any level on the tissue proneness to develop a T1-visible lesion.
The average distance of the T1-lesioned tissue from the ventricles was higher than the one of the T1-spared tissue.

Conclusion. Our results suggest that an higher density of neurites seem to play a role on the probability of development of a T1-visible WM lesion in MS, while the orientation dispersion of the axons does not appear to have any impact on these pathological events.
An higher coherence and compactness of structure in the myelin-rich WM areas could constitute a facilitating factor for the auto-inflammatory immune process against myelin antigens.
It is interesting to see that this effect, which appears already significant when considered the whole brain, looks to be even more prominent in the “deep WM layer”, which is the furthest-from-CSF part of WM.
Conversely, the lesion-promoting effect of high ND seems to be attenuated or neutralized in the WM layers neighboring the CSF: this fact brings to speculate the existence of some underlying interaction between inflammatory soluble factors and tissue structure, at different WM deepness levels.

2 . Background

2.1 . Magnetic resonance imaging

The phenomenon of magnetic resonance (MR) of the atomic nuclei is known since its discovery in 1946 by the Nobel-prized Bloch and Purcell.[1, 2]
A rapid evolution followed, which brought to development of wide-bore superconducting magnets (around 35 years ago), which permitted the technique to be applied in clinical settings, following the first human MR images realized in Nottingham and Aberdeen in 1980.[3]
Nowadays, with the availability of uncountable pulse sequences fitted for different applications in neurologic disorders, magnetic resonance imaging (MRI) is considered to have become an unsubstitutable and powerful diagnostic instrument.

2.1.1 Diffusion weighted imaging

Diffusion weighted imaging (DWI) is an advanced branch of MRI sciences, currently experimenting an active evolution.
The basic physical principle of diffusion weighted imaging is the random “Brownian” displacement of water molecules in the analyzed sample.
In a pure fluid solution, motion of water molecules is completely free in any direction; the amount of displacement in time mainly depends on the temperature of the solution, with no directional

preferentiality: this is named “isotropic diffusion”, and can be observed, for example, in the cerebro-spinal fluid (CSF).
Instead, when diffusion of water molecules is subject to structural constraints in the biological sample (for example, impermeable cells membranes), the diffusion phenomenon is limited and the amount of displacement in the same period of time will be reduced: this is termed “restricted diffusion”, and the amount of slowdown of molecular displacement is also influenced by cito-histological features and cell wall integrity. For example, a higher diffusion restriction is observed in highly-packed cancerous cells compared to normal tissue
When the shape and the disposition of the cells assumes a fibrillary micro-tubular structure, the constraints to water diffusion act mainly on the transversal plane of the fibers, causing the diffusion to happen more intensely along the main axis of the fibers: this phenomenon in which water diffusion is not equal in all directions is called “anisotropic diffusion” and is observed, for example, in the neurite-rich regions of the brain, i.e.: white matter (WM) tracts.

Studying the amount and characteristics of diffusion in human tissues is precious for many diagnostic purposes, from oncology to ischemic stroke, and is made possible by a specialized MRI pulse sequence, called DWI.[4]
To obtain an image contrast based on the different rate of diffusion between different tissues, a conventional spin echo sequence must be modified by adding “diffusion gradients”: these two gradients are applied before and after the 180° pulse, equally distanced in time from it, both having the same duration and the same (but opposite) amplitude, hence the first operating a “dephasing” action, the second a “rephasing” one.

The sequence is designed in a way that, if no movement of particles happen in the lapse of time between the application of the two diffusion gradients, the effect of the second gradient suppresses completely the effect of the first one and there will be no signal loss. Since in biological tissues there is a certain grade of proton diffusion, the rephasing performed by second gradient will be incomplete and this will generate a signal attenuation on the diffusion weighted image.

The b-value of a diffusion sequence is a number, which is dependent on three factors: the time between application of the two diffusion gradients, their strength and their duration

A mathematical relation between the same sequence repeated with (b-*n*) and without (b-*zero*) any diffusion gradient applied, allows to purify the component of the signal deriving from true diffusion effects from the ones deriving from the underlying conventional pulse sequence, and, thence, to create an image which is weighted on diffusion only, called “apparent diffusion coefficient” (ADC) map.[5]

2.1.2 Diffusion tensor imaging

A more recent technique, called Diffusion Tensor Imaging (DTI), is derived from the classical diffusion weighted imaging and estimates diffusion of protons along multiple directions, by the application of multiple non-collinear directional-sensitizing diffusion gradients, to allow a virtual reconstruction of a diffusion tensor for each imaged voxel. For the fitting of a diffusion tensor, a minimum of 6 directions of analysis is required, but an increasing number of directions assures more robust fittings.

Technically: similarly to as seen in the DWI, one or more “baseline” acquisitions with a b-value of zero are always essential - aside to the directionally sensitized ones - to assure the diffusion weighting of the sequence. When analyzing WM with classical DTI, the b-value of 1000 is considered to be the most accurate for the directionally sensitized acquisitions. Anyway, it is possible (and sometimes useful) to add directional diffusion acquisitions with different b-values in the same sequence; in this case, each group of directional diffusion acquisitions with the same b-value is considered a “shell”.[5]

DTI is particularly valuable in anisotropic diffusing areas, such as the WM of the brain, permitting to simulate tractography and fiber tracking and to quantify the characteristics of the axonal microstructure via four distinct scalar measures: fractional anisotropy (FA, which corresponds to the normalized variance of the tensor’s eigenvalues), mean diffusivity (MD, the average of the eigenvalues), axial diffusivity (AD, the major amongst the three eigenvalues) and radial diffusivity (RD, the average of the two smaller eigenvalues).
Thanks to DTI’s mathematical simplicity and its sensitivity to subtle changes in WM structure and integrity, innumerable scientific works are employing DTI with the objective of better understanding the normal anatomy of WM pathways and of improving the diagnosis and the pathogenesis knowledge on several neurological and psychiatric affections, such as multiple sclerosis (and other demyelinating diseases), axonal traumatic injuries, brain neoplasms, epilepsy, ADHD, bipolar disorder, schizophrenia, neurodegenerative diseases, etc.[5]

2.1.3 Advanced diffusion imaging techniques

As mentioned before, there are situations where the classical model of DTI encounters some critical issues, and appears largely insufficient to explain the complexity of the normal structure and the impairments of human brain tissue. One of the typical failures of the classical DTI model is when dealing with regions of the brain where the fibers are crossing in multiple directions or are taking short radius turns.

Some of these shortcomings are surmountable by employing diffusion imaging methodologies which require an increased complexity, either in the acquisition phase (A) and/or in the post-processing algorithm (B):

A – a typical example is the acquisition of multiple shells, each shell with a different b-value (with some b-values even larger than 2000), in order to sensitize the signal to diffusion restriction and to different spans of molecular displacement profiles.

B – the most representative example is the employment of "compartmental modelling"[6]

Here (Figure 1) is a synthetic representation of the most relevant advanced diffusion MRI techniques in use in research contexts, classified as suggested by Pasternak et al., 2018.

Figure 1

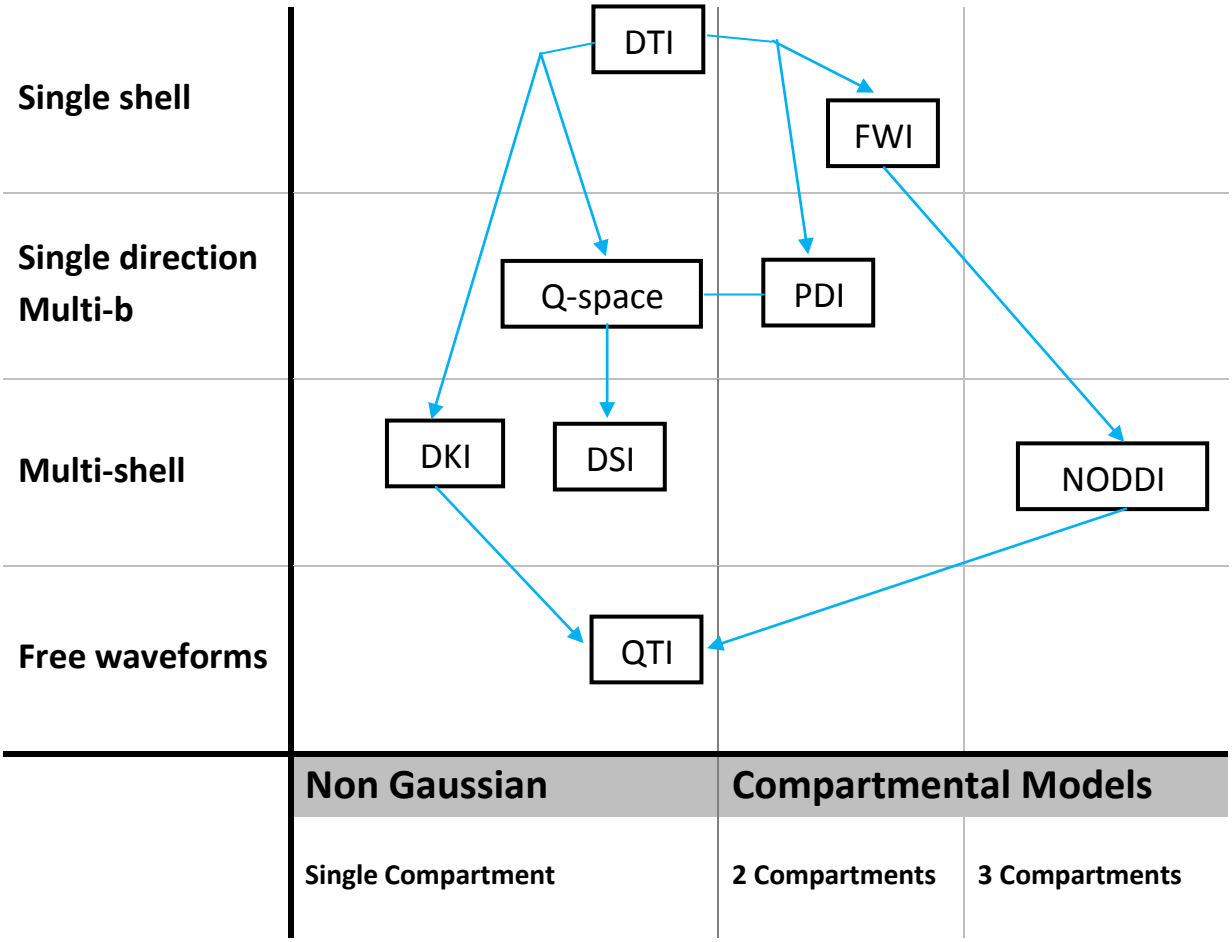

The methods belong to two main families: on the left the ones not based on a model, but obtained by measures of deviation from a Gaussian distribution; on the right the ones based on a tissue compartmental model. From top to bottom the classification reflects an increasing acquisition complexity, from left to right it reflects an increasing modelling complexity.

DTI = diffusion tensor imaging
FWI = Free-water imaging
PDI = Permeability-diffusivity imaging
DKI = Diffusion kurtosis imaging
DSI = Diffusion spectrum imaging
NODDI = Neurite orientation dispersion and density imaging
QTI = q-space trajectory imaging.[6]

Advanced diffusion imaging techniques can be divided in into two main groups, depending on the analysis approach: model-based and non-model-based.

- The non-model-based group, which relies on the sole analysis of the signal without needing to assume an underlying tissular model, includes Q-Space Imaging, Diffusion Kurtosis Imaging, Diffusion Spectrum Imaging and Q-space Trajectory Imaging.
- In the model-based group, a compartmental tissue model is defined “a priori”, subdividing the biological sample in multiple pools of water molecules with different diffusion properties; subsequently an estimation of the microstructural characteristics is run separately in each distinct tissue compartment. Free Water Imaging, Permeability Diffusivity Imaging, Neurite Orientation Dispersion and Density Imaging (NODDI), and Q-space Trajectory Imaging belong to this last group of methods.[6]

We will now concentrate on the description of the NODDI diffusion analysis method and omit the discussion of the other systems, as they fall outside the arguments of this thesis.

2.1.4 Neurite orientation dispersion and density imaging

The neurite orientation dispersion and density imaging (NODDI) method, is based on a three compartmental model (Figure 2), featuring an intracellular, an extracellular and a free-water partitions.

The free-water section (i.e.: CSF, perivascular spaces, interstitial water, plasma, etc.) is considered as isotropic and modelled consequently, with a diffusion coefficient corresponding to the one of pure water at body temperature ($3\times10^{-3}mm^2/s$).

The intracellular compartment treats about the fluids confined inside the axonal membranes, which present a strongly restricted radial diffusion, and is simulated by a bundle of cylinders with zero radius ("sticks") and with a fluid diffusion along the longitudinal axis considered as constant and set to $1.7\times10^{-3}mm^2/s$. A mathematical function, originally a Watson distribution with two free parameters, puts in relation the mean orientation of the sticks and their dispersion around that mean axis. The estimation of neurite density is obtained from the fractional volume of this second compartment.

With the extracellular partition, the model takes in account the inter-axonal spaces, which are supposed to have a not restricted diffusion, but hindered along the same axis of the intracellular sticks. This compartment is therefore modelled using beams of tensors with equal orientation dispersion to the axons. A function is posed to regulate the neurite dispersion, their density and the parallel diffusivity of the sticks with the longitudinal and transversal diffusivity of the tensors.

With these premises, the model keeps four free parameters: the orientation dispersion index (ODI), the neurite density (ND), the free-water isotropic fraction (ISO) and the axonal mean orientation.[7]

Figure 2

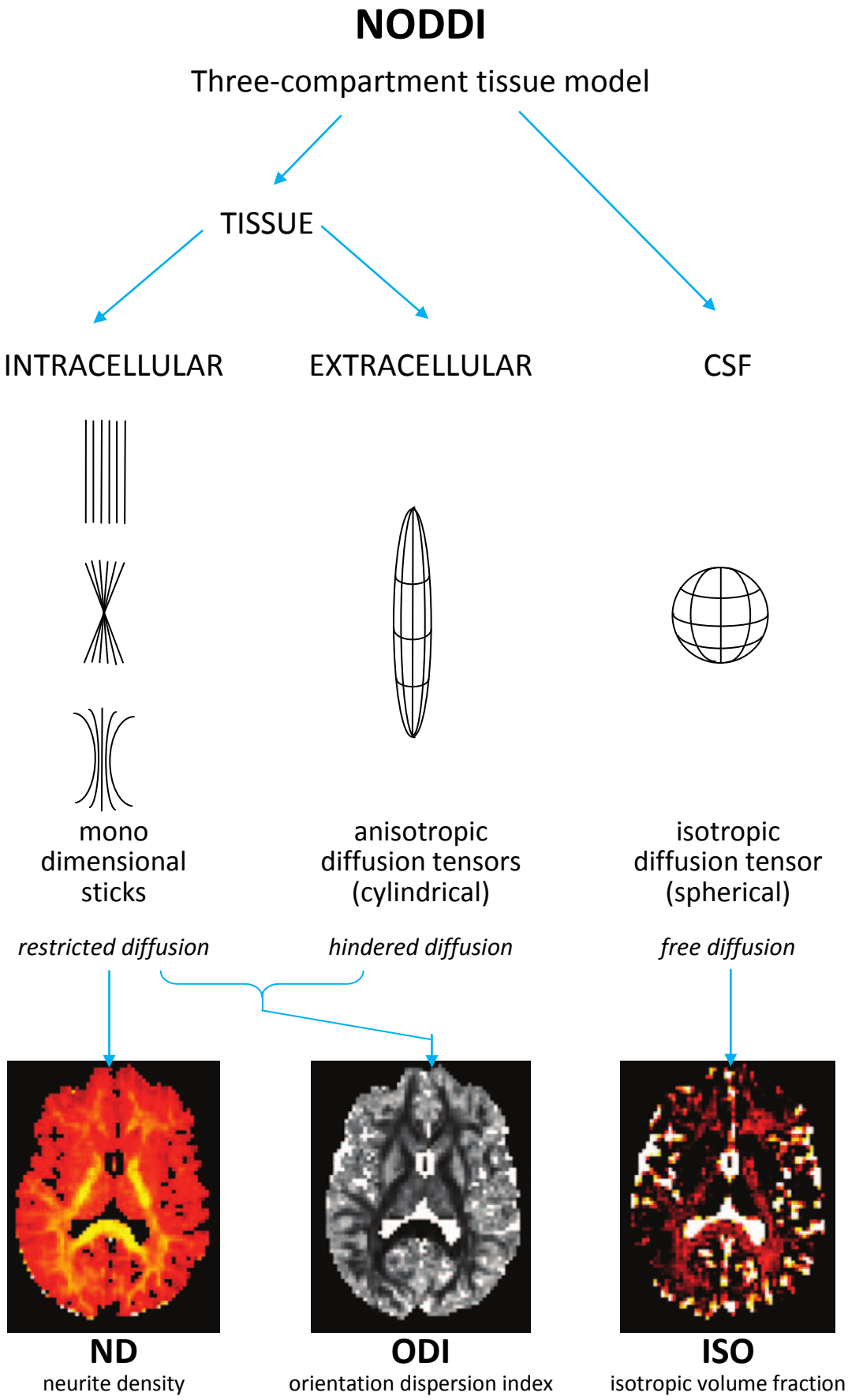
NODDI
Three-compartment tissue model
TISSUE
INTRACELLULAR
EXTRACELLULAR
CSF
mono dimensional sticks
anisotropic diffusion tensors (cylindrical)
isotropic diffusion tensor (spherical)
restricted diffusion
hindered diffusion
free diffusion
ND
neurite density
ODI
orientation dispersion index
ISO
isotropic volume fraction

NODDI (Neurite orientation dispersion and density imaging) is based on a three-compartment model, an intracellular compartment (with restricted diffusion), an extracellular one (with hindered diffusion) and a CSF compartment (with free diffusion): the model allows the elaboration of parameter maps, known as neurite density (ND) map, orientation dispersion index (ODI) map, isotropic volume fraction (ISO) map.[8]

As mentioned above, the NODDI model, to be run, needs an expressly tuned diffusion acquisition protocol, with at least two shells: for example, a set of directions should have a b-value of around 1000, the second set (higher number of directions to compensate the signal noise) should have higher b-values (2000 or above).
Here are some technical details of typical acquisition protocols (these are examples, but NODDI can adapt to different options):

- 1.5T magnet, 11 b=0 basal images, 3 shells (9 directions at b=300, 30 at b=800, 60 at b=2400), isotropic voxel resolution 2.5mm, TR 8900ms TE 99ms.[8]

- 3T magnet, 5 b=0 basal images, 3 shells (30 directions at b=1000, 30 at b=3000, 30 at b=4500), isotropic voxel resolution 2mm, TR 12000ms TE 108ms.[9]

To sum up, NODDI, comparing to the classical DTI method (which provides a mere FA information), gives the opportunity to specify if the microstructural WM modifications are due to an actual loss of neurite density or just to an augmented orientation dispersion of the axons.
This makes the neurite density index a potential sensitive marker of demyelination (despite its low specificity); the orientation dispersion parameter, instead, which reflects crossing and bending fibers, could prove to be a useful marker in the study of neuronal developmental or neuronal degenerative diseases.[7]

DTI and other advanced tractography techniques are currently in use in the Human Connectome Project, which has the objective to build connectivity maps of the normal human brain at a parcellated/regional level.[10]

2.2 . Post-processing information technologies

2.2.1 Ubuntu LINUX – based operating system

Ubuntu is an operating system which was firstly released in 2004; it is based on the stable kernel LINUX, more precisely on the DEBIAN branch.
The name Ubuntu is derived from a south-african zulu philosophical word which means “humanity towards the others”, a concept that expresses the foundation of each human being upon the contributions of all the other human beings.
Ubuntu is, indeed, an open-source operating system, mainly composed by free software (protected by the GNU General Public License), but also supporting commercial software.
A new release is available every 6 months, and a “long term support” version every 2 years. The updates are developed and managed by the British company “Canonical Ltd.”, with the collaboration of a large community of developers, whose work is organised under a meritocratic model system.
The project is economically supported by sale of Ubuntu-related premium support services and by the installation of the system on commercial hardware objects.[11]
Due to its stability, gratuity, compatibility and customizability, Ubuntu is very well suited for running university software libraries for MR image analysis and its terminal is ideal for batch-scripting; these reasons made it our first choice to be used in the data processing phase of our project.

2.2.2 Windows operating system

Windows is a widely spread commercial operating system, firstly developed in 1985 by Microsoft as a graphical shell for MS-DOS, and subsequently becoming a dominator in world's market share for personal computers.[12]
In our project, Windows (NT 10 version) was useful to run the image processing phases requiring Matlab.
Moreover, Windows NT 10 environment allows to run several proprietary software which are essential for the management of the numerical results of the image processing and for their statistical analysis.

2.2.3 BASH scripting language

BASH is a Unix command language developed for the GNU project and first released in 1989, as an improvement to the syntax of the already existing Bourne Shell. The acronym of the name means "Bourne Again SHell".
BASH shell comes with a command processor, i.e.: the user types commands in a text-only window, and each command corresponds to an action. Instead of typing commands one-by-one, a list of commands can be read and executed by BASH from a script file in format ".sh" (Figure 3). This function is of paramount importance when batch-analyzing hundreds of MR images from multiple patients.
As well as for Ubuntu, BASH is free software, published by the Free Software Foundation and protected by the terms of the GNU General Public License.[13]

2.2.4 FSL image processing tool library

FSL is a software library (extended name: Functional magnetic resonance imaging of the brain Software Library) comprehensive of multiple tools (all running in BASH environment) for the analysis of MR images of the brain and the subsequent statistical analysis of deriving data.
FSL include tools to process different MR methods, such as morphological-structural MRI, functional MRI, DTI.
FSL is developed, updated and made publicly and freely available – for research and non-commercial uses – by the Functional MRI Analysis Group of the University of Oxford.[14]
Some MRI processing tools of FSL relevant to this project are, for example, the Brain Extraction Tool (BET), the FSL Automated Segmentation Tool (FAST), the FSL Linear Registration Tool (FLIRT), the MRI image reviewer (FSLView), etc. (Figure 3).
Furthermore, some BASH FSL commands were core in this project (Figure 3): for example, “FSLstats” allows to convert MR images to numerical data; “FSLmaths” gives the opportunity to perform mathematical operations between MR images.

Figure 3

```
cd '/media/analisi/580E2AE30E2AB9C0/Niccolo/0_Dottorato_Piaggio_Noddi'
#
#
#
#
echo -e '\n\n_____INIZIO_SCRIPT_____'
local_rootdir=$(pwd)
usbdsk_rootdir='/media/analisi/NP_Ricerca2/0_Dottorato_Piaggio_Noddi' # scommentare se uso il disco NP_ricerca2 come Disco Di origine Dati
#usbdsk_rootdir='/media/analisi/NiccoloPiaggioRicerca_1/_Niccolo_Ricerca_Backup_HP/0_Dottorato_Piaggio_Noddi' # scommentare se uso il disco
echo -e 'Cartella locale:\t\t'  $local_rootdir
echo -e 'Cartella dell HDD esterno:\t' $usbdsk_rootdir
#
#
#
echo -e '\n\n_____INIZIO_TABELLA_____'
    echo -e '\n\n\033[41mPATIENT NUMBER\033[0m\t\t\033[41mNum Voxel con Errori\033[0m\n'
for pz_folder in $(find $local_rootdir/Output -name 'MGH*all' -type d | sort -n) ; do
#
    pz_ID=$(basename "$pz_folder")


#
    cd $pz_folder
#
    n_pixel_error=$(fslstats results_NODDI_error_code.nii -V | cut -d' ' -f1)
    if [ "$n_pixel_error" -eq "0" ]
    then echo -e $pz_ID'\t\t\033[0;32m'$n_pixel_error'\033[0m'
    else echo -e $pz_ID'\t\t\033[0;31m'$n_pixel_error'\033[0m'
    fi
#
    cd $local_rootdir
#
done
#
echo -e '\n_____FINE_TABELLA_____\n\n'
#
echo -e '\nAlcuni pazienti sono da revisionare...\n \033[0;31mQuale vuoi aprire?\t\033[0;32m(Input SOLO le ultime 2 CIFRE dell ID del PZ)\03
read pz_to_open_num
pz_to_open_folder="MGH_10${pz_to_open_num}_all"
echo -e 'Apro il Paziente: '$pz_to_open_folder
#
#
for pz_folder2 in $(find $local_rootdir/Output -name ${pz_to_open_folder} -type d | sort -n) ; do
#
#
    cd $pz_folder2
    fslview -m ortho \
    NODDI_DWI.nii \
    results_NODDI_odi.nii \
    results_NODDI_kappa.nii \
    results_NODDI_ficvf.nii \
    results_NODDI_fiso.nii \
    results_NODDI_fmin.nii \
    results_NODDI_error_code.nii -l Red
    cd $local_rootdir
#
done
#
```

Extract from a BASH script expressively written for this project and actually used in it, including FSL commands, to review and validate the processed images.

2.2.5 Matlab scripting platform

MATLAB (shortening for MATrix LABoratory) is an environment for numerical calculation and statistical analysis, written in C, including its own programming syntax, developed by MathWorks.[15]
MATLAB offers the opportunity to visualize functions and data, implement algorithms, create customized graphical user interfaces, manipulate matrices and bridge with other programs.
These last two features were particularly sought in our project to be able to handle with 3-dimensional and 4-dimensional matrices (MR images) and to interface with the NODDI diffusion imaging toolkit, described below.
MATLAB is employed by millions of people in the industry and university worlds, thanks to its uncountable supports to different research fields, and to its compatibility to most operating systems, such as Windows, MAC OS, GNU/Linux and Unix.[15]
The version of MATLAB used in our project is R2016B, the one currently made available by the University of Genova IT department.

2.2.6 NODDI diffusion imaging toolkit

The diffusion MRI processing software used in our project is "NODDI Matlab Toolbox", an extension for MATLAB built by UCL Microstructure Imaging Group.
The toolbox allows to obtain NODDI parameter estimation maps from a double-shell high angular diffusion MRI sequence, exploiting parallel computing and the three-compartmental tissue geometric model described above in detail.

The software adapts to an acquisition protocol optimized for clinical feasibility, and requiring a 30 minutes average scanning time.

The output parameter maps thus obtained are:
- neurite density map,
- orientation dispersion index map,
- CSF volume fraction map,
- fiber orientation in the 3-dimensional space maps,
- map of fitting objective function vales,
- map of the concentrated parameter of Watson distribution used to compute orientation dispersion,
- map containing information about errors occurred during the fitting process.

The parameter maps are able to highlight microstructural properties of the cerebral WM and grey matter (GM) which are much more specific than those of the classical DTI analysis method.[16, 17]

2.2.7 SPSS statistical data analysis interface

Statistical Package for Social Sciences is a commercial software by IBM with an extensive suite of statistical analysis functions.
It features both a graphical user interface and the scriptability option for data analysis.
Due to its characteristics it is one of the most widespread computed statistical tools available.[18]

2.3 . Multiple Sclerosis

Multiple Sclerosis (MS) is a chronic multifocal auto-inflammatory disease which affects the myelination of the central nervous system (CNS).

2.3.1 Classification

The first acute episode of neurological impairment, usually involving the optic nerve, brainstem, spinal cord and cerebellum, lasting for a minimum of 24 hours before the clinical recovery, is referred as “clinically isolated syndrome” (CIS).
The most common variant of the disease shows multiple episodes of inflammatory focal demyelination of the CNS, in some cases associated to a clinical neurological deficit, interlapsed with periods of clinical remission; this form, known as “relapsing remitting” (RR) MS, affects 85% of the patients.
RR MS, in 15-30% of the cases, evolve to a “secondary progressive” (SP) disease, where the neurological impairment is escalating and leads to a cumulative disability.
In a minor part of cases (10-15%), MS advances towards disability, with no relapses, directly since the onset: in this case we assist to a “primary progressive” (PP) MS.[19]

2.3.2 Epidemiology

MS is the main demyelinating disorder in developed world and the second most common etiology of permanent disability in young adults (after traumatic CNS injuries). Average age at diagnosis is 30 years.[20] Global prevalence of the disease is estimated at around 31 per 100000; prevalence in Europe is higher, with 127 per 100000. A significant correlation between MS prevalence, latitude and socio-demographic index was found.[21] The prevalence showed a trend to increase in the last 20 years, due to the lengthening of survival, the improvements in diagnosis, and the change of diagnostic criteria.[21, 22]

Global incidence is rated at 2.5 per 100000; European incidence is 3.8 per 100000.[23]

Gender ratio female:male for MS was considered to be unfavorable for males at the beginning of last century, but an overturning of this measure was observed in the last period. This apparent rise of gender ratio could reside in various factors: a better access to healthcare for women in modernity and the higher prevalence, in females, of MS subtle forms which can be better detected with current diagnostic criteria and MR imaging.[23, 24].

Statistics on mortality show that survival rate after 25 years accounts around 70-88%, while survival time ranges between 24 to >45 years. Mortality decreased by 11.5% in the last 20 years.[21, 25]

Favorable prognostic factors on survival and quality of life are: RR variant, earlier clinical onset (between 25 and 30 years of age), first neurological episode with visual or sensory symptoms, fewer disability accumulated in the first year of disease, longer lag between the first and second relapse.[26]

2.3.3 Risk factors

It is not possible to isolate a single etiology explaining development of MS: multiple factors appear to play a role, both congenital and environmental.

Only three environmental factors detain an evidence of unbiased, consistent association with MS: presence in serum of immunoglobulin G versus the nuclear antigen of Epstein Barr virus, infectious mononucleosis, smoking. Several associations between MS and other risk factors were explored, but showed to be light or inconsistent: vaccinations, biochemicals, dental amalgam, past traumatic events or surgeries, atopy, eczema, impaired venous flow, vitamin D deficiency.[27, 28]
Interaction of environmental factors triggering the disease could be represented by molecular mimicry, surface cell exposure of new autoantigens, peripheral dispersion of normally CNS-segregated autoantigens, pro-inflammatory cytokine setting.
For example, it was proposed that Epstein Barr virus could activate B cells inside the CNS or provoke a generalized imbalance of the immune system.[29]

Genetic context has a significant impact in MS: monozygotic twins are both affected with a 25.9% concordance, while dizygotic ones only with 2.3%.[30]
Some variants of the HLA gene of the major histocompatibility complex were identified to have a predisposing action towards MS (HLA-DRB1*15:01 allele, diffuse in European population), or a protective effect against MS (class I HLA-A*02:01 and class II DRB1*14:01).[31]

More than one hundred of transcriptional polymorphisms in genes encoding for interleukin-7 and -2 receptors were found to show correlation with MS pathogenesis, probably inhibiting the tolerance systems or lowering the immune cell activation threshold. Different levels of expression of immunological-chain-related genes in MS patients seem to influence the aggressiveness phenotype of the disease.[29, 32]

2.3.4 Pathogenesis

MS is an auto-inflammatory process targeting the CNS. The classical pathological feature of MS is the presence of inflammatory focal lesions, more frequently localizing in the perivenular spaces, with an interruption of the blood-brain barrier which allows lymphocyte infiltrate, glial activation, myelin sheath loss and, eventually, neurite disruption with impairment of neuronal signaling.[33]

Generalizing, MS sets off in congenitally predisposed individuals who underwent some kind of triggering environmental factor which cause an autoinflammatory reaction against the CNS. It is not easy to identify why the first inflammatory process begins and how the immune system sustains it.

A theory states that the first encounter between antigen and T cells is in the periphery, and then activated lymphocytes and monocytes move to the CNS. The second explanation is that a primary event occurs intrinsically to the CNS (viral infection, neurodegeneration…), provoking a local immune reaction which releases CNS antigens to the systemic blood flow, and eventually attracting autoreactive immune cells.[34]

The second hypothesis is supported: by the limited effect of available medicaments in the progressive forms of disease, and by the apparent independence between the relapse recurrence and the cumulative neurodegeneration; both facts seem to confirm an underlying primary neurodegenerative process which is separated from the inflammatory manifestations.[35]

In any case, a CNS-antigen-based immune response is activated and CNS is invaded by lymphocytes. In consequence, microglia is activated, contributing to tissue damage and sustainment of the disease. Inflammatory processes are visible at any phase of MS, mainly in the acute, but also in the chronic ones. Immune cell infiltrates localizing in the perivenular space are hallmark of disease, and contain: macrophages, T cells (CD8+ > CD4+), B cells and plasma cells. Oligodendrocyte and demyelination appear consequently to inflammation. In the progressive forms of MS, the immune reaction involves more extensively the CNS, with diffuse demyelination, neurite loss, microglia activation, development of tertiary lymphoid structures and cortical injury. The result of this is a progressive WM and GM trophicity decrease, due to a loss of neurites and neuronal bodies, which is the basis of irreversible clinical disabilities in MS.[29]

2.3.5 Pathology

The microscopical appearance of the focal lesions features primitive demyelination, followed by glial scaring, neurite and neuronal body degeneration and loss.
Lesions localize mainly in WM, but also in cortical and nuclear GM, brainstem and spinal cord.
A certain degree of remyelination is observed in focal lesions. Lesions can be classified in: acutely active-, chronically active-, slowly expanding-, inactive- lesions or remyelinated "shadow plaques".
Either if cortical lesions are hardly identified in MR in-vivo technique (only in 10-15% of cases), they appear extensively diffuse in pathology specimens of MS.
In many cases, a lesion extends from cortex to the underlying subcortical WM, in others the lesions are purely intracortical or subpial.
Superficial cortical lesions show meningeal inflammation and tertiary lymph follicles associated, especially in progressive MS forms.

It is relevant to this thesis to note that active demyelination begins on cortical surface and propagates with a superficial-to-deep gradient. The subsequent degeneration involves neurites and cellular bodies.
The involvement of deep gray matter with focal lesions and diffuse neuronal degeneration is precocious in disease history, but evolves slowly over time.
"MR normally appearing" WM and GM are instead characterized by a diffuse injury at a micropathological level, especially in progressive MS stages.

WM damage is characterized by inflammatory infiltrates surrounding small vessels, diffuse axonal involution, glial activation and astrocytic scars. In the progressive phases of disease, the increasingly severity of demyelination in cortex, with neuronal body loss, brings a further neurite depletion in the WM.[33]

2.3.6 Clinical features

Clinical manifestations following active plaques in MS can vary widely, since they depend on the geography of lesions in the CNS: typical onset acute symptoms are unilateral optic neuritis, partial myelitis or brainstem syndrome.[36]
Conversely, the chronic progressive neurodegeneration manifests heterogeneously with slowly worsening symptoms (in order of frequency, from more to less common): asymmetric paraparesis, hemiparesis, cerebellar ataxia, visual loss or dementia.
The speed of evolution of the clinical course is very variable; prognostic indicators of disability accumulation have been associated to gender, brain atrophy, age and degree of disability at diagnosis.

2.3.7 Diagnosis

Since a single test is not sufficient to provide a specific diagnosis of MS (not even tissue biopsy), the diagnosis must be reached by integration of multifactorial data (clinical, laboratory and MRI).

Specifically, a dissemination of the disease in time (DIT) and a dissemination in space (DIS) must both be demonstrated to identify an actual MS case.

The latest revision of the McDonald diagnostic criteria was codified in 2017[37], and bases the diagnosis of MS upon objectivable DIT and DIS of the CNS lesions, plus the consideration and exclusion of alternative better explanations for the clinical symptoms.

This current diagnostic criteria revision still allow a purely clinical diagnosis; nevertheless, it is undeniable the increasing role of MRI in diagnosing MS. For example, a single MRI scan could satisfy both criteria: DIT (contemporaneous presence of Gadolinium enhancing and non-enhancing lesions) and DIS (simultaneous involvement of multiple foci in CNS, such as supra- and infra-tentorial or spinal cord).

Moreover, MRI is a precious tool to exclude many MS-mimicking conditions.[37-39]

CSF specimen testing, though not usually necessary, can support the early MS diagnosis if demonstrating the presence of oligocolonal bands (DIT criteria) when the DIS criteria is already clinically satisfied. Other CSF features compatible with MS are a normal to moderately rise in cell count (<25 cells per cm^3, mainly lymphocites), a low protein level (<1g/L), a raise in IgG index and an absence of serum oligoclonal bands.

Finally, neurophysiological evoked potential testing on optic, sensory and auditory pathways could help the identification of subclinical lesions in the CNS, thus potentially confirming the DIS criteria.[37]

2.3.8 MRI studies in MS

The key MRI feature of MS is the presence of multiple focal inflammatory lesions, visible as hyperintense in T2 and Fluid Attenuated Inversion Recovery (FLAIR) weighted sequences and hypointense in T1 imaging.
Preferential localizations of lesion are periventricular and subcortical WM and infratentorial structures.
Lesion load (LL), correlates with the burden of clinical disability (standardly measured with the expanded disability status scale EDSS).
Spinal cord is affected by a MRI detectable lesion in 90% of MS patients and in 50% of CIS patients.[40]
The MRI visible lesion burden in CNS alone is not enough to explain all the disability in MS, thus defining a gap between clinical and imaging features.
In order to optimize diagnostic power and disease progression surveillance, guidelines have been redacted to codify the most accurate MRI protocols.[41, 42]
In addition to classical pulse sequence standard protocols, some more sophisticated MR techniques have been introduced with the aim of better understanding, in vivo, the pathophysiological processes which bring to the development of MS.
For example, employing a high-resolution delayed-post-gadoliunium FLAIR scan, MR is capable of demonstrating leptomeningeal inflammation and tertiary follicles in up to 50% of the cases of MS, on a clinical magnet, and in up to 90% on a ultra-high field magnet.

Magnetization transfer ratio maps are able to unveil the diffuse demyelination process underlying the normally appearing WM in the standard pulse sequences.

Spectroscopic MR, giving insight on the content of N-acetyl-aspartate, and MR Sodium imaging proved to detect neuronal body and axonal degeneration.

Neurodegeneration is even measurable indirectly by means of brain tissue atrophy, which proved to be particularly relevant in deep GM nuclei and to correlate with EDSS.[43]

Despite several possible biasing factors, brain and spinal cord atrophy is measurable (cross-sectionally and longitudinally) on 3D T1 MR images.[44]

Plenty of literature flourished around resting state functional MRI in MS patients, with stimulating findings, but which are beyond the interests of this thesis.[45-49]

Some studies combining structural connectivity data collected from diffusion sequences with the functional connectivity collected by functional MRI, with brain atrophy data and/or with clinical scores, found (sometimes univocally, sometimes with contrasting results between papers) that structural disconnection could provoke an increase in functional connectivity in MS patients[50, 51] or a re-modulation of the functional networks[52-54], with a final exhaustion of the compensatory connectivity systems in the latter stages of disease.[55]

Concerning pure DWI MR techniques, plenty of literature studied MS pathology under the micro-structural, meso-structural and macro-structural aspects.[56]

Microstructural studies

More than 300 DTI-based papers regarding MS were published, finding abnormal DTI parameters in MS lesions (reduced FA and increased MD, RD, AD)[57, 58], thus demonstrating increased water content together with myelin and axonal loss and glial scarring.

Compared to healthy controls, even normally appearing WM of MS patients present a diffuse abnormality in DTI parameters, consistent with the fact that MS damage spreads beyond the visible borders of classical MRI visible plaques.[57, 58]

In GM, the results were more controversial[59-62], partially for the simplistic limitations of the DTI model.[63]

Although on animal models it was evidenced that AD and RD values reflect respectively axonal injury and myelin disruption[64, 65], it is not prudent to generalize this conclusion.[66, 67]

Despite the rich literature on classical DTI in MS, its parameters are very “raw”, since they are derived from the assumption of a Gaussian water diffusion model[68], which hardly captures the actual microstructural properties of the cerebral tissue, and can be biased by innumerable factors.

Model free algorhythms, such as Q-Space Imaging and Diffusion Kurtosis Imaging promise to match with more fidelity the physical and cytological properties of the biological sample, such as the axonal diameter.[69] Unfortunately, the acquisition protocols for these approaches are complex and time-demanding and hardly applicable to clinical settings[70]: up to now, studies were limited to post-mortem imaging-vs-histology validation[71, 72] or to animal MS models[73, 74], and there are few published papers that prove their usefulness in small numbers of in-vivo MS patients.[75-83]

A few Diffusion Spectrum Imaging studies on post-mortem samples successfully validated this imaging technique metrics on histological stains.[84, 85]

Surprisingly, although multi-compartmental models such as NODDI were developed expressly to be practicable in clinical settings, to date there are no in-vivo MS published studies.[7]

Summing up, various basic or advanced diffusion MRI techniques helped to provide biomarkers of tissue damage which improve specificity and sensibility of conventional MRI imaging: diffusion imaging techniques allow to visualize subtle and early changes in normally appearing brain tissue or to highlight the pathogenethical differences between similarly-looking WM lesions.

As a drawback, most diffusion microstructural biomarkers lack of specificity if compared to actual histology, potentially presenting identical diffusion MRI alterations despite being due to a coexistence of multiple different etiological substrates.

Mesostructural studies

Focal MS microstructural damage does not have local consequences only: due to the structure of brain, it happens to localize along neuronal pathways and networks, impairing their function at a mesoscopic scale. This is why the mere study of lesion load and microscopical tissue properties is not sufficient to explain the clinical disability burden of MS.[86]

To address this issue, diffusion MRI tractography was developed: a system to simulate axonal bundle pathways by analyzing, voxel by voxel, the diffusivity pattern and direction of the WM and therefore estimating and reconstructing virtual "tracts".

Classical DTI measurement can thence be acquired within the tract boundary, and be eventually associated with a specific clinical deficit.

With this "tract based" system, motor and sensory pathways were object of the most conspicuous number of investigations in MS, thanks to their easier comparison to eloquent manifestations and to clinically measurable criteria (i.e.: EDSS, timed walk test, etc.).

Corticospinal tract (CST) consistently shows alteration of the DTI values (AD, RD, MD) in MS patients, if compared to healthy subjects, and this CST damage was associated to functional impairments in clinical scales and atrophy (thinning) of the primary motor cortex. Conversely, FA anomalies of the CST seem to have a lesser impact on disability.[87-89]

Plastic changes and reorganization of the primary motor cortex were demonstrated and in MS patients with lesions affecting CSTs unilaterally, by comparing tractographic connectivity with morphological (surface area) data.[90]

In alternative to the single-tract method, contemporary multiple-tract based analysis are made possible by means of the "graph

theory": this mathematical method is applied to MS neurophysiopathology by defining some GM regions as "nodes" and their pairwise WM inter-connections as "edges". Each edge is obtained by multi-seed-region tractography and is characterized by its own DTI properties. This wide-area approach allowed defining integrity and efficiency metrics on a more extended network, which appear to more satisfactorily explain the EDSS burden of disability in MS patients.[86, 91-93]

In addition, besides the sensory-motor domain, other more complex aspects of MS neuronal symptomatology (such as fatigue, memory and processing speed) could be studied by applying these sophisticated methods to a wider range of brain structures, such as cingulum.[94, 95]

However, there are some drawbacks that currently suggest caution in the use of this network-level method in clinical settings: loss of information of the original precise localization of the WM lesions and risk of amplification of the well-known pitfalls of tractography.[96]

Macrostructural studies

Again, the structural connectome is a system based on the graph theory; this time, however, the full brain is more broadly considered as a complex integrated network, with distinct functional areas (GM nodes obtained from cortical and subcortical structural MR parcellation) connected by axonal wiring (WM edges reconstructed non-invasively on the base of diffusion MRI data).[97-102]

Its metrics does not help us to fill the gap between MS microhistological features and imaging, but have potential to give us a deep insight on how neuronal communication brings to human behavior and how its dysfunction bring to disease.[103, 104]

Connections between each couple of GM areas can be weighted by different metrics: the number of streamlines simulated with tractography[105], the tract's diffusion MRI parameters[106], or any other microstructural MR metric of interest[107]. A point of strength of this approach is, indeed, its ability to summarize in a few number of easily manageable measures a very complex ensemble of pathological effects, and it constitutes a promising base from which to furtherly analyze local alterations on the more traditional mesoscopical and microscopical level.

Various papers reported in MS an early alteration of the structural connectome, with an initially regular functional network preservation[108, 109]; this pattern was found opposite in other primary neurodegenerative diseases, such as Alzheimer's.[110, 111]

An overall brain network efficiency in RR MS patients was linked to disruptive changes in several meso-scale sub-networks an eventually to disability.[112] Localization of WM damage, if

compared to the efficiency rate of the whole network and the clinical performance status of the subject, gives an opportunity to better understand the level of tolerance of each subnetwork to injury.[113]

Methods of connectome analysis are relatively recent and still under active development, and still require validation under several technical aspects: for example, there is not unanimity consensus around which method to use to parcellate the cortex, how to realize the tractography or which are the correct metrics to weight the graph's edges.[114]

Conversely, connectomic analysis could unveal some subtle widespread cross-subnetwork alterations, invisible on the traditional mesoscopic and microscopic levels, and independent from the focal origin of injury.

In conclusion, diffusion MRI techniques, despite their physical and technical limitations and their difficult applicability in clinical settings, consent a good degree of multimodality and a wide range of valid parameters for research purposes in MS. Additionally, they give the opportunity of integrating neuronal damage complementary information collected from different points of view on a progressive scale of magnification, from the macroscopical level, to the mesoscopical and to the microstructural one.[56]

2.4 . The Sys4MS consortium study

The Sys4Ms multi-center study lies in the wider context of the European Union supported ERACOMED project, a research program on MS based on “system medicine”.

This approach exploits and integrates, by advanced computational tools, the information gathered by multiple biomarkers, such as imaging, clinical data, and “multi-omics”.

The final aim of the project is to better explain pathology and pathogenesis of MS, at a “patient-by-patient” level, in order to develop personalized treatments.

329 MS patients were recruited cross-sectionally, along with 90 healthy controls. All patients underwent brain MRI and optical coherence tomography; clinical scores were calculated, the type of MS treatment in use was recorded. Blood samples were analyzed by multi-omics approach (genotyping with around 500.000 genetic markers, cytomics with 17 antibodies targeting immune cell subpopulations, phosphoproteomics on white blood cells at 3 time points with 20 kinases).

Significant differences were unveiled between patients and controls at multiple levels of biomarkers. The information gathered from a such large number of biomarkers gives us the opportunity to compute an integrated profile of the disease, a promising value which clarifies the prognosis and help the development of objective decision systems to optimize MS management.[115]

2.5 . The Human connectome project repository

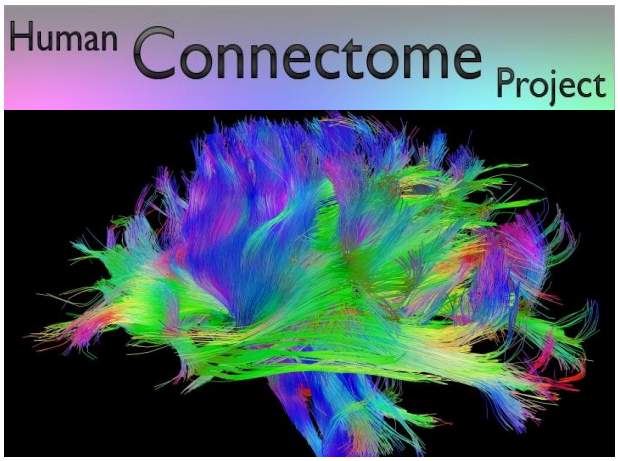

The Human Connectome[97] Project was conceived in 2009 and involves two research consortia for a total of 16 research institutes, including Washington University in Saint Louis, University of Minnesota, Oxford University, Harvard University, Massachusetts General Hospital, the University of California Los Angeles and D'Annunzio University of Chieti–Pescara.[116]

In particular, the WU-Minn-Oxford consortium was able to collect, via the most advanced MRI 3T and 7T hardware and software systems available, a massive database of ultra-high quality structural and HARDI diffusion MRI brain data, from around 1200 healthy adults, plus hundreds of data from twins and siblings[117], and made it publicly available and downloadable from the internet in an open-source platform.[118]

This huge data repository is a precious base which allowed to build an unprecedentedly-defined connectome map of human brain, shedding light on WM pathways organization[119]; its public availability permitted to develop hundreds of research studies on various subjects, including dyslexia, autism, Alzheimer's disease, and schizophrenia.

Acquisition of MRI data on human young healthy brains is still in progress; in addition, some research centers of the consortia are focusing on populations different than young adults or on subjects affected by a particular disease. This will help to understand the changes occurring in brain connectivity structure during ageing or caused by neurologic pathologies.

3 . Thesis Introduction

3.1. Multiple Sclerosis Lesion “Geography”

To date, despite a whole century of research efforts, the basis of WM damage spatial localization (lesion appearance and lesion evolution) in MS are poorly understood.[120]

Although it is recognized that the entire brain is affected by pathological processes of MS, it is however well known that not all the anatomical structures of the brain are affected at the same degree[121]: it was observed, both via ex vivo and later via in vivo MRI experiments, that lesions and normal appearing WM changes are more frequent and intense in the WM and GM adjacent to the outer (i.e. subpial)[122] and inner (i.e. ventricular)[123] surfaces of the brain.

The brain parenchyma underlying the subpial brain surface is reported to be an elective site of localization for cortical lesions, which appear to be consistently present in subjects with PP MS.[124]
The presence of subpial cortical damage was related to meningeal inflammation, in all MS subtypes, suggesting the possibility that the presence of soluble inflammatory factors in CSF could facilitate the spatial distribution of tissue damage to the outer layers of superficial GM.[125]

Similarly, while it is well established that the lesion formation process appears to predilect the periventricular WM structures[123], recent studies added the notion that even extra-lesional WM anomalies are more intense in the regions immediately underlying the ependymal ventricular surface[126].

In addition, a diffusion weighted imaging study in subjects with PP MS demonstrated an association between cortical lesion load and the severity of periventricular normal appearing WM damage, suggesting that a common factor could play a role in the development of both cortical lesion and periventricular normal appearing WM abnormalities in PP MS.[127]

Some recent studies sought to explore the correlation of deep and superficial brain damage in relapse-onset MS, and found associations between periventricular WM lesions and the entity of cortical atrophy.[128] Other studies highlighted that in relapse-onset MS, both in subependimal[129] and in subpial[122] structures a decreasing gradient of normal appearing WM anomalies is present, thus suggesting that a common facilitating factor could underlie tissue damage in both cortical and periventricular areas.

Most of these observations, however, did not find a etio-pathological explanation yet.

3.2. Imaging Recent Advances

As discussed above, the degree of damage found in the brain structure has been classically assessed by measurements gathered via diffusion weighted imaging (i.e.: fractional anisotropy, mean diffusivity, axial diffusivity and radial diffusivity)[5] or via magnetization transfer imaging.
Some novel advanced diffusion MRI protocols and analysis models permit a further characterization of the tissular microstructure, overcoming some limitations of the classical models, especially when sampling areas where several WM fiber and bundles are not directionally coherent but “cross” the sampling voxel in different directions.[6]

One of the most promising approach which come in help in these cases of “crossing fibers voxels”, where the classical models fail, is Neurite Orientation Density and Dispersion Imaging (NODDI) model.[16]
The NODDI modeling requires a targeted DWI acquisition with an optimized protocol with at least two-shells.[16]
The NODDI MRI protocol was developed with the scope to obtain a “non-invasive histology”, avoiding patient discomfort and possible side effects of standard biopsy-histology procedures and enabling temporal monitoring through repeat measurements.
Moreover, microstructure imaging produces maps over the whole brain rather than a targeted biopsy sample of a few mm3, so is less prone to false negatives from poor targeting, and provides a more complete picture of heterogeneous diseases, such as MS, which affect very heterogeneously the different brain areas.[130]

This “microstructure imaging” (i.e. a technique for estimating fibre orientations and configurations from diffusion MRI enabling non-invasive studies of brain connectivity through tractography) works by fitting mathematical models of cellular architecture to imaging data.[7]

The NODDI algorithm produces separate maps of dispersion of fiber orientations (how much fanning/bending/etc.), fiber density, and partial volume with free water (e.g. CSF). The traditional fractional anisotropy (FA) index from diffusion tensor imaging (DTI) confounds these three effects; NODDI allows a separate analysis of each. Moreover, the technique provides useful information in GM as well as WM. In GM, the dispersion and density of dendrite orientations provides contrast between functional areas that translates into contrast from the diffusion MRI signal. NODDI requires only 10-30 minutes acquisition time with standard pulse sequences, therefore is clinically feasible.[7]

The key advance in NODDI’s fitting technology compared to the previous DWI analysis techniques is to move away from voxel-by-voxel estimation of microstructure parameters to exploit spatial coherence: microstructure is usually similar in proximal voxels so it is possible to pool data to improve estimates and reduce noise in the measurement. It was demonstrated in simulations that assuming consistency of microstructure along fiber tracts, it is possible to improve microstructure parameter estimates, and resolve long-standing ambiguities in tractography, such as kissing versus crossing.[131]

Various tools were developed to validate NODDI microstructure imaging applications:

- a diffusion simulation system that supports arbitrary tissue environments, from packed cylinders with diameters reflecting WM to arbitrary mesh models derived from confocal or electron microscopy images[132];

- WM phantoms from specially designed meshes or glass capillaries[133-135];

- an asparagus as a biological phantom with similar pore structure to WM[134];

- a viable tissue chamber to allow imaging of excised tissue in in-vivo conditions for ten hours or more[136];

- an ex-vivo histological verification by comparison of the NODDI parameters of a mouse brain acquired on a 7T MRI scanner and its transparent-rendered dissections.[137]

3.3. Rationale

Spatial localization of WM T2 / FLAIR hyperintensity in multiple sclerosis along the brain has been extensively studied and is well known; though, the reasons that cause the evolution from early MS lesion (i.e. T2 / FLAIR hyperintensity) to chronic lesion (i.e. “black hole” on T1 sequences) remains poorly understood.

Specifically, it is not clear why some lesions evolve to black hole and some others not.

Two hypothesis are posed:

- the distance from CSF could represent a determinant factor to lesion evolution via inflammatory facilitation

- some pre-existent regional properties of the WM microstructure make the tissue locally more prone to structural degeneration and lesion evolution

3.4. Objectives

The overall aim of this project is to better explain the relationship within the gradient-like centripetal distribution of tissue damage in MS and the anatomical microstructural properties (NODDI's neurite density, orientation dispersion index, CSF volume fraction, fiber orientation) of the affected WM, and hence better explain the spatial preferentiality and the pathogenesis and evolution of the MS plaque.

3.5. Project Plan

Our research developed along this timeline of work organization:

1. The first step of these three years of doctorate has been gathering normal anatomical data on a large pool of healthy subjects (as made publicly available by the Human Connectome Project Consortium) and therefore building, via NODDI modelling mean parametric maps of a normal population in order to assess the different properties of tissue in relation to anatomical localization.

2. The second step was to cross-sectionally evaluate the lesion geography on a cohort of MS patients, defining WM T2/FLAIR hyperintensities and black hole localization.

3. The third step was to search whether the NODDI microstructural WM properties in the corresponding location of black holes on normal brain maps is predictive of lesion formation and or black hole degeneration.

4. The fourth step was to evaluate at which “deepness” (i.e.: distance from the CSF-brain interface) the effects of the NODDI microstructural WM properties have the strongest effect on the probability of T2-to-T1 lesion evolution.

5. The fifth step was to check if, in our sample of patients, the mean distance of T1 lesions from ventricular CSF was significantly different from the mean distance of the rest of the non-T1 affected parenchyma.

4 . Research - Step 1

"NODDI modelling"

4.1. Population

Data was acquired from healthy adults between the ages of 20 and 59. Demographic information, including gender and age range, are shown in Table 1.

Table 1

N	M:F ratio	Age (mean, STD)
35	19:16	37.60 ± 12.71

Demographics of the Human Connectome Project population

The participants gave written consent, and the procedures were carried out in accordance with the institutional review board approval and procedures.
Each dataset (in nifti format) consists of a Magnetization-Prepared Rapid Acquisition Gradient Echo (MPRAGE) scan, a high resolution T2-SPACE scan and diffusion scans with 4 different b-values.

4.2. Methods

The DWI scans were post processed and the NODDI model was fitted by NODDI toolbox (MIG, UCL Microstructure Imaging Group) extension for Matlab (The MathWorks, Inc.) and NODDI WM microstructural properties maps were generated for fiber orientation, intracellular volume fraction (ficvf also known as “neurite density” ND), isotropic volume fraction (fiso), and orientation dispersion index (ODI).

4.3. Results

The maps obtained from one of the subjects are shown in the image below (Figure 4).

Figure 4

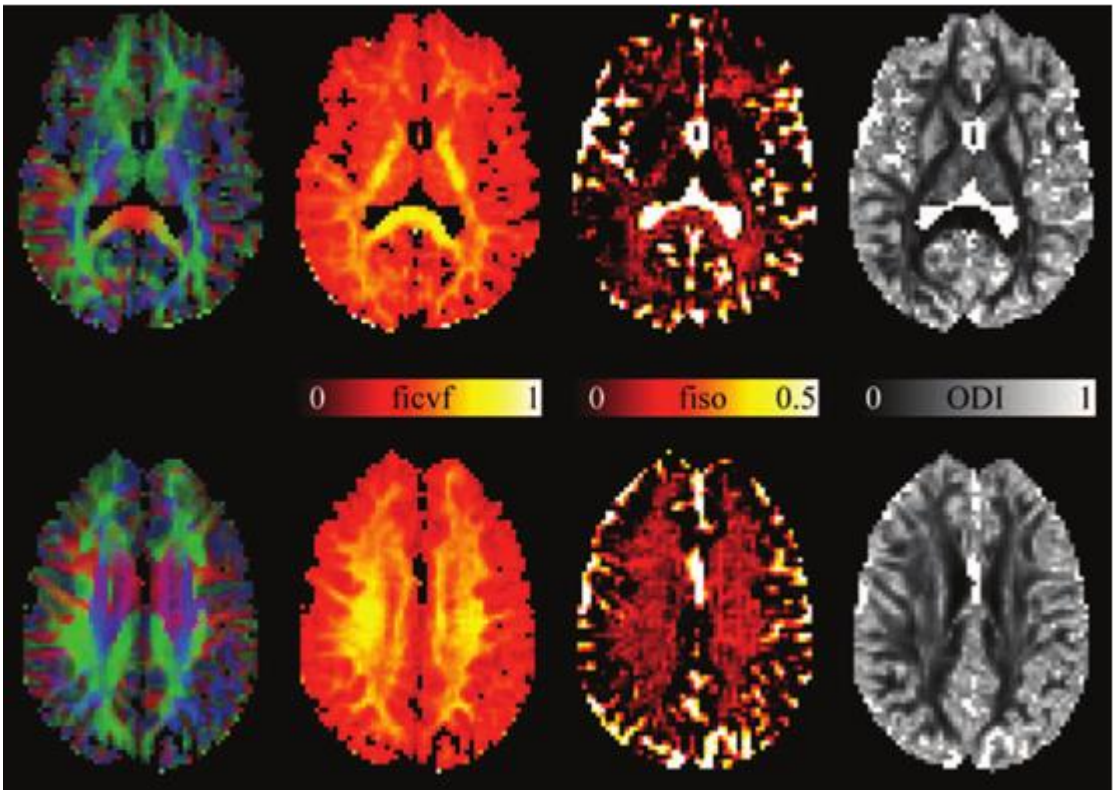

Parametric maps obtained from NODDI modelling, from left to right: the axonal mean orientation, the neurite density (ficvf), the free-water isotropic fraction (fiso) and the orientation dispersion index (ODI).

Values of ficvf (neurite density) are high in neurite-rich areas such as WM, as can most clearly be seen in the internal capsule and the splenium of the corpus callosum. The fiso maps accurately highlight the ventricles and surrounding CSF that have a very high isotropic diffusivity. The orientation dispersion index (ODI) maps the dispersion of neurites around the principal diffusion direction. In single-fiber regions in the WM, this can be regarded as an indication of the coherence of the axons in that voxel. This can most clearly be seen in the posterior limb of the internal capsule, wherein the ODI is low indicating high axonal coherence.

The normal brain NODDI microstructural properties maps thus obtained were translated in a normal MNI space[138-141]

via “NiftiReg” (NiftyReg is an open-source software for efficient medical image registration developed by members of the Translational Imaging Group with the Centre for Medical Image Computing at University College London, UK), and the “mean maps” were computed for each parameter.

These maps thus obtained are generally of great interest if used as a “normal brain microstructural atlas”, since they potentially allow to assess, in any white-matter-damaging disease, how the WM microstructure of an average normal brain “should be”, in the region where a lesion disrupted the tissue and consequently the WM structure is no longer evaluable.

5 . Research - Step 2

"MS Coort Recruitment and Analysis"

5.1. Population

For our work we recruited 92 MS patients.

The participants gave written consent, and the procedures were carried out in accordance with the institutional review board approval and procedures.

Patients were recruited in the context of the Sys4Ms consortium, a multicenter, multidisciplinary study with the aim to develop new tools based on systems medicine to improve and personalize the management of MS patients. The consortium is developing mathematical models into which clinical information MRI and omics data from diverse sources can be integrated and which can be used to generate algorithms that can predict the disease course and future disability in specific subgroups of MS patients, as well as aid the selection of the best therapy for each individual.

Our population anagraphics are depicted in Table 2.

Table 2

MS Subtypes	RR	PP	SP	TOT
N	68	11	13	92
M:F ratio	18:50	5:6	4:9	27:65
Age (mean, STD)	40.01 ± 10.27	50.63 ± 7.31	52.15 ± 6.49	43.55 ± 10.71
EDSS (median)	1.5 (0 - 6)	4 (4 - 6)	4 (2 - 6.5)	2 (0 - 6.5)

Demographic and disease information of the University of Genova Sys4MS subpopulation enrolled in this study.

5.2. Methods

Patients underwent, aside to several clinical and Immunological tests, a 3T MRI scan which included the following high resolution pulse sequences (Figure 5): 3D T2, 3D FLAIR; 60 directions DWI; Resting State blood oxygen level dependent (BOLD) imaging; pre and post contrastographic 3D T1.

The scanning protocol lasted approximately 1 hour. Motion blurred sequences were repeated.

Figure 5

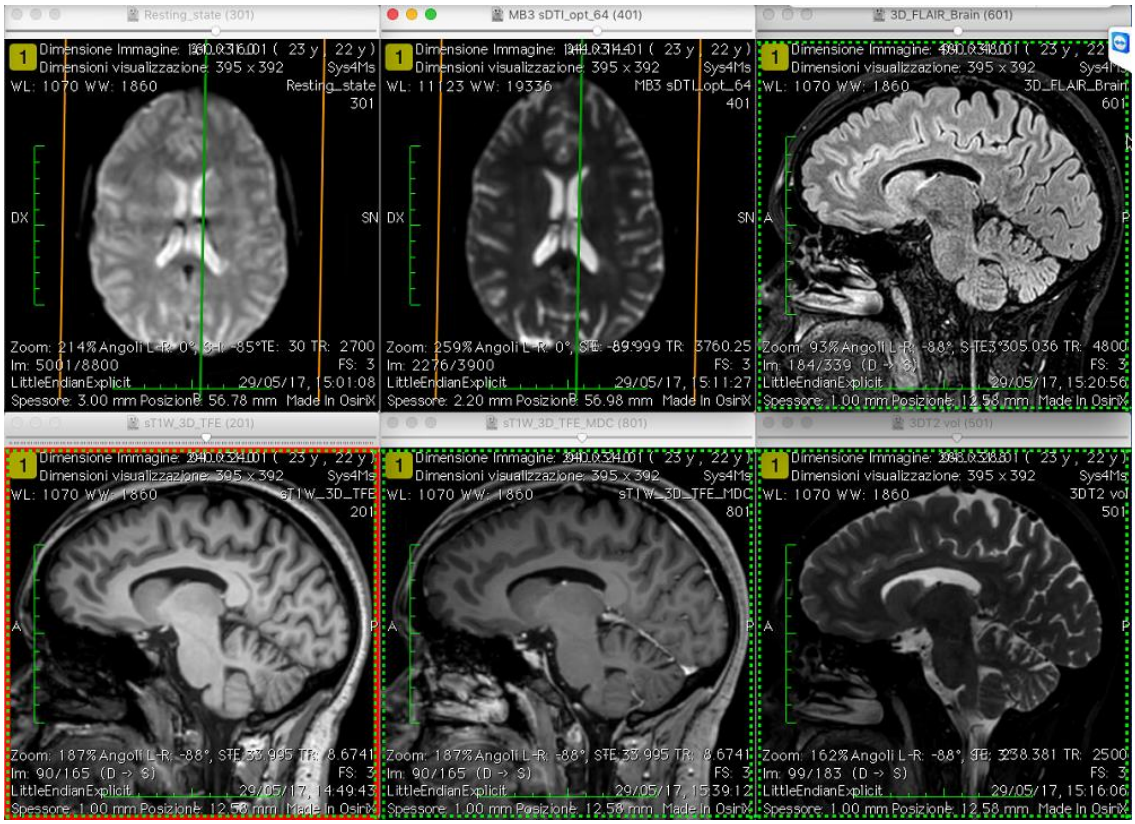

The MRI scan protocol employed in the University of Genova Sys4MS study, including: Resting State Functional MRI, 60-directional single-shell DTI, 3D FLAIR-weighted imaging, pre- and post-contrastographic 3D T1-weighted imaging, 3D T2-weighted imaging.

3D FLAIR and 3D T1 volumes were post processed by resampling to 3mm axial slices in order to make the manual drawing of the lesions possible.

Lesion edge contours were traced, slice by slice, using an active surface semi automatic algorithm using the software “JIM” (version 6, Xinapse Systems).

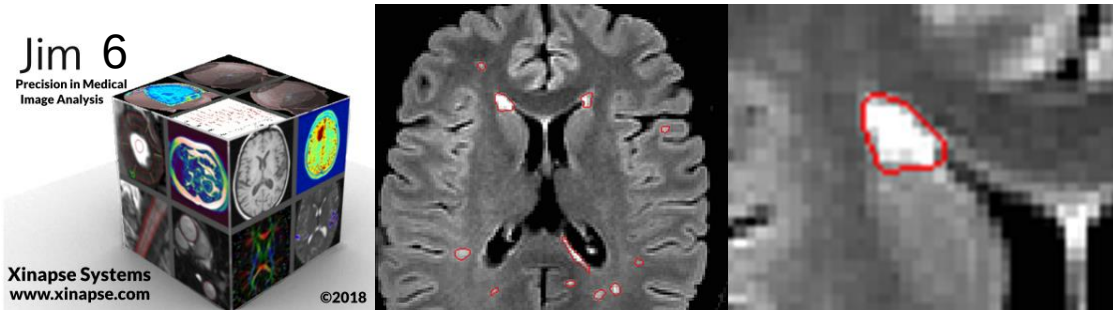

Each segmentation result underwent a double accuracy check (including a revision by an experienced neuroradiologist) and, if necessary, manual edited.

Figure 6 shows an example of lesion segmentation respectively on FLAIR hyperintensities ("LesionT2Map") and on T1 black holes ("LesionT1Map").

Figure 6

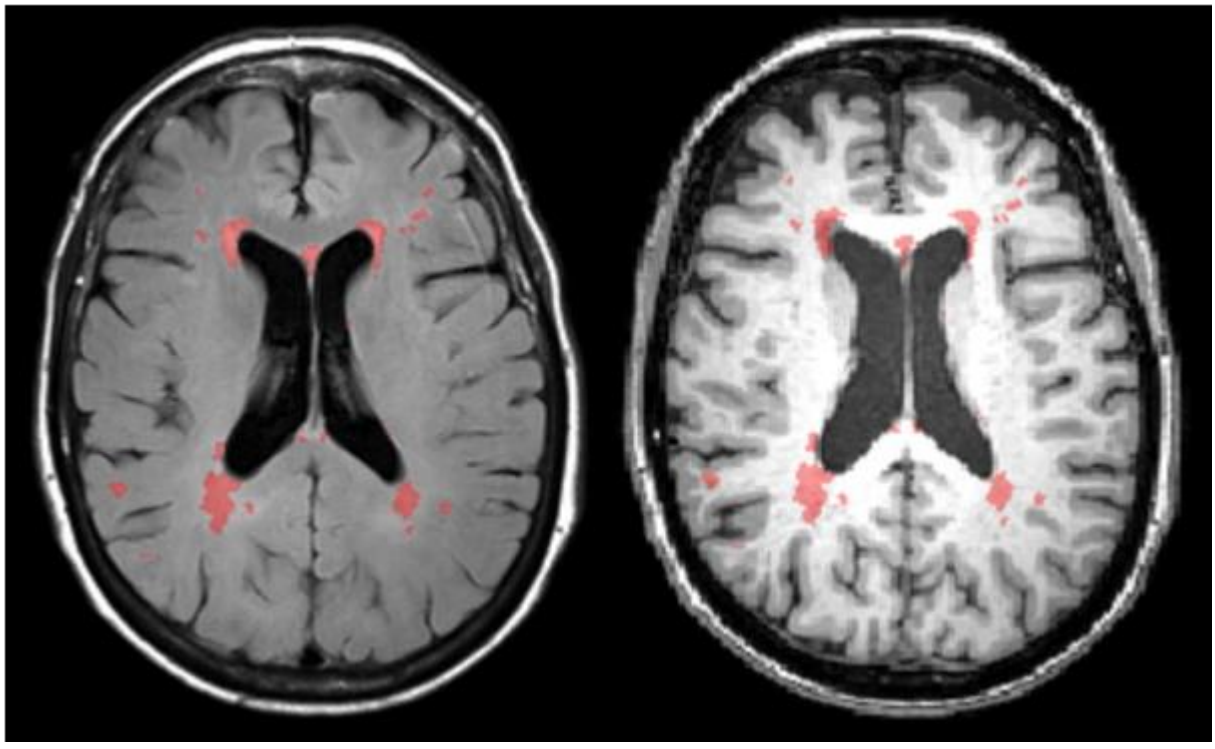

Semi-automatic neuroradiologist-revised lesion segmentation of the 3-mm axially reformatted 3D-FLAIR (on the left of the image) and 3D-T1 (on the right) images of one of the patients' brain.

The binary “LesionT1Map” and” LesionT2Map” of each patient were furtherly computed to obtain binary “LesionNonT1Map” (i.e.: a map of the “T2 only” lesions, therefore with a voxel value 1 on each voxel where a T2 lesion was detected but a corresponding T1 lesion was NOT present, and value zero elsewhere) and a binary “NormalWhiteMatterMap” (i.e.: voxel value 0 for T1 and/or T2 lesions and value 1 for all the remaining WM voxels untouched by any lesion).

The lesion maps thus obtained were translated in a normal MNI space[138-141] via “NiftiReg” (NiftyReg is an open-source software for efficient medical image registration developed by members of the Translational Imaging Group with the Centre for Medical Image Computing at University College London, UK).

5.3. Results

Lesional Load for each map was evaluated in each patient, as shown in the Graph 3 below.

Graph 3

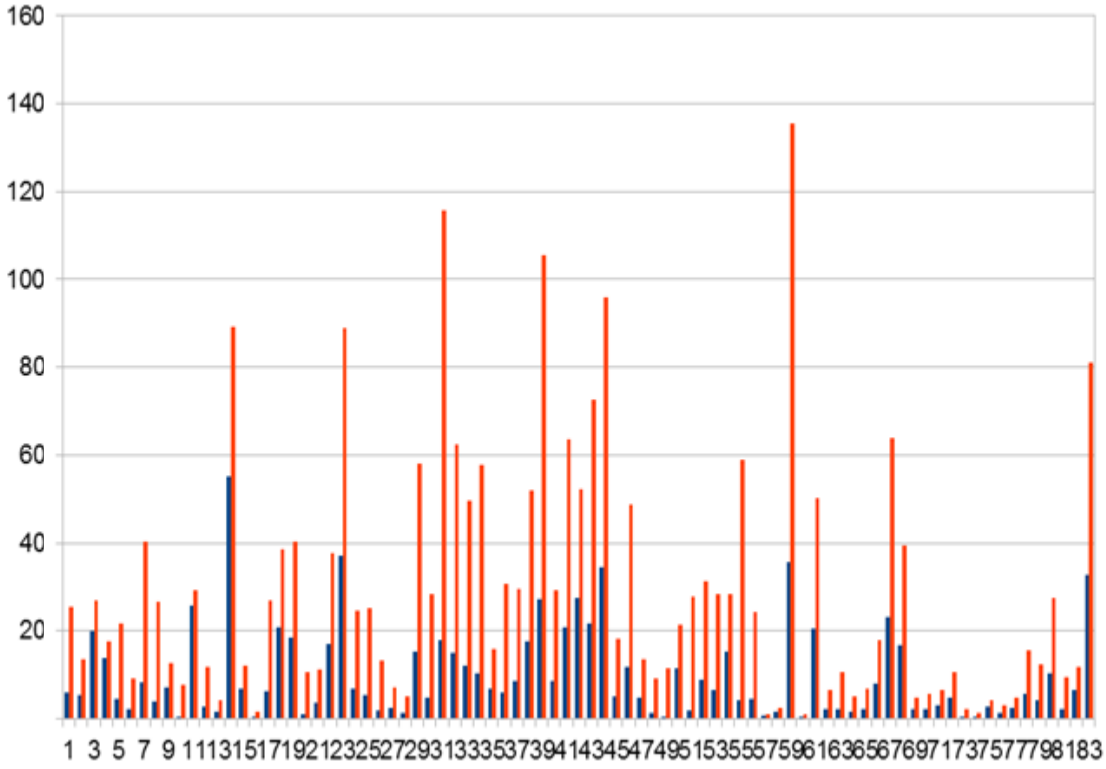

X axis = Patient identifying number,
Y axis = Lesion Load (total volume) in milliliters,
Blue column = T1 lesion load,
Red column = T2 lesion load.

6 . Research - Step 3

“Correlations Between NODDI Microstructural Properties and Lesion Masks”

The search of correlations between NODDI microstructural WM properties and lesion masks was performed via two different approaches, *Experiment A* and *Experiment B*.

6.1. Experiment A

Via a patient-by-patient approach:

METHODS

Firstly, we extracted for the whole brain of each patient the mean value for each noddi parameter inside the “1-valued” voxels of each binary LesionT1Map, LesionT2Map, LesionNonT1Map and NormalWhiteMatterMap.

Then, we performed a general linear model test to explore the eventuality of a possible predictivity of a black hole formation via the “a priori” knowledge of the noddi microstructural properties of a determinate anatomical region of the brain. Statistical correction was included for: lesion load, disease duration, age.

RESULTS

Here we present the descriptive statistics (mean and standard deviation) for the NODDI parameters found in each subcategory of WM status. Since we performed statistical tests on the results regarding the T1 lesion regions of interest, compared to the non-T1-affected regions, and we did not take in consideration the normal WM and T2 lesion maps, due to the objective of this study, we will present descriptive statistics regarding the first couple of regions of interest only.

Average ODI and ND were found to be respectively 0.291 ± 0.031 and 0.618 ± 0.030 in the T1 affected regions.

Conversely, in the T1 lesion-free brain, these parameters measured respectively: 0.285 ± 0.022 and 0.612 ± 0.029 (see Table 4).

Table 4

WHOLE BRAIN	ODI	T1-lesioned	0.291 ± 0.031	] p=0.675
		T1-lesion-free	0.285 ± 0.022	
	ND	T1-lesioned	0.618 ± 0.030	] **p=0.014**
		T1-lesion-free	0.612 ± 0.029	

Summary table displaying results of Orientation Dispersion Index (ODI) and Neurite Density (ND) mean values (± standard deviation) in "T1-affected" versus "T1-spared" brain areas, calculated on the whole brain.
On the right, significance of the (lesion load, disease duration, age corrected) general linear model test for each couple of values.

No significant difference was found in ODI parameter between T1-lesioned areas and T1-lesion-free areas.

Instead, a significant difference exists when comparing the mean ND parameters of the same regions (p=0.014).

6.2. Experiment B

Via a voxelwise approach:

METHODS

We generated a single large 4-dimensional matrix containing for each voxel two essential information: 1- the lesion probability value in that voxel position for our SM patient's sample (LesionT1Map, LesionT2Map, LesionNonT1Map and NormalWhiteMatterMap), and 2 - the value of the noddi parameter in the corresponding voxel in the healthy subject's noddi parameter maps. The purpose of this action should have been to evaluate the correlation between the mean noddi value and the probability of lesion for each area of the brain.

RESULTS

Unfortunately, the size of the matrix thus obtained was too massive to handle due to some of our actual hardware-software limitations: this road looks promising although challenging but we hope to be able to overcome this issue in the next future.

7 . Research - Step 4

"Correlations Between NODDI Microstructural Properties and Lesion Distance from the CSF"

7.1. Methods

We evaluated at which "deepness" (i.e.: distance from the CSF-brain interface) the effects of the NODDI "a priori" known microstructural tissue properties (as offered by the previously computed normal tissue mean NODDI parameter maps) have the strongest effect on the probability of T2-to-T1 lesion evolution.

To do this, we divided the brain maps into three "deepness" layers, each measuring an equivalent thickness, namely, from deep to superficial (Figure 7): "periventricular WM" (shown in blue in the "B" image), "deep WM" (in green) and "subpial layer (in red); we derived these layers from the 12-layer-map described by Pardini M et al, 2016 ("A" in the image).

We coregistered all the layer maps to the normal MNI space[138-141] and then multiplied the binary lesion maps with each of the three layer-selection maps. We subsequently calculated the mean and standard deviation ODI and MD parameter for each layer in T1-lesioned areas and T1-lesion-free areas.

Finally, we performed a general linear model test, corrected as described above, to investigate differences between NODDI parameter mean values at each level.

Figure 7

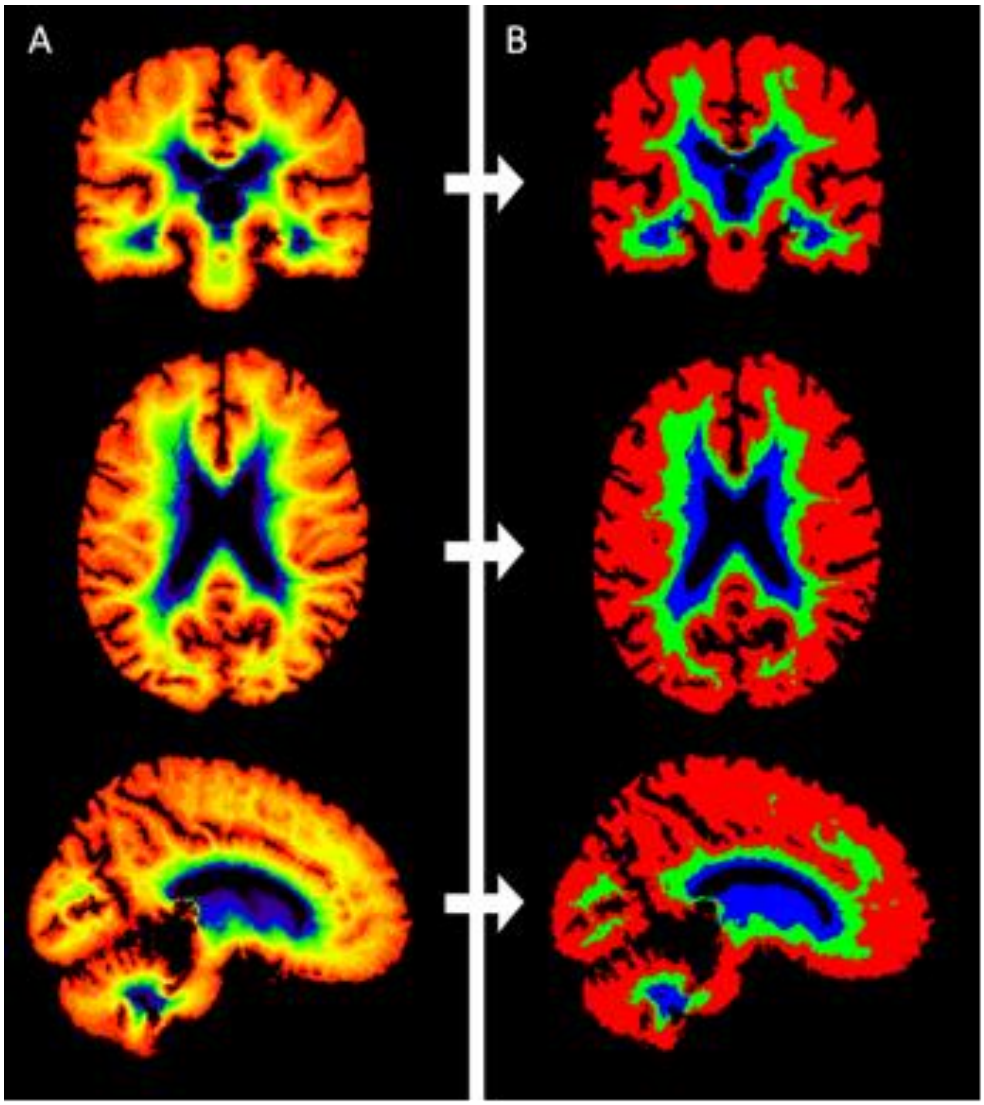

A (left side) - depicts the 12-layer-white-matter-deepness map described by Pardini M et al, 2016

B (right side) - displays the simplified three-layer-white-matter-deepness map that we derived from the one on side A; color code of the layers:

- BLUE: "periventricular WM",

- GREEN: "deep WM",

- RED: "subpial layer.

7.2. Results

Here (Table 5) we show descriptive statistics for each parameter, as described in this methods section; on the right we show the general linear model correlations between the results in the T1-affected and T1-not-affected regions of interest. In our sample of patients, we found significant correlation (p=0.004) only in the deep WM layer, when comparing the neurite density values of the T1 affected with the T1 normally appearing regions of interest.
A close-to-significant p-value was found for orientation dispersion values in the subpial layer.

Table 5

PERI VENTRICULAR WHITE MATTER	ODI	T1-lesioned	0.285 ± 0.040	] p=0.855
		T1-lesion-free	0.278 ± 0.027	
	ND	T1-lesioned	0.604 ± 0.037	] p=0.561
		T1-lesion-free	0.609 ± 0.034	
DEEP WHITE MATTER	ODI	T1-lesioned	0.264 ± 0.034	] p=0.501
		T1-lesion-free	0.265 ± 0.021	
	ND	T1-lesioned	0.649 ± 0.034	] **p=0.004**
		T1-lesion-free	0.629 ± 0.033	
SUBPIAL LAYER	ODI	T1-lesioned	0.320 ± 0.067	] p=0.053
		T1-lesion-free	0.329 ± 0.036	
	ND	T1-lesioned	0.600 ± 0.123	] p=0.153
		T1-lesion-free	0.596 ± 0.050	

Summary table displaying results of Orientation Dispersion Index (ODI) and Neurite Density (ND) mean values (± standard deviation) in "T1-affected" versus "T1-spared" brain areas, calculated at three different deepness levels of the white matter (See Figure 7).
On the right, significance of the (lesion load, disease duration, age corrected) general linear model test for each couple of values.

8 . Research - Step 5

"T1 Lesion Load Distance From CSF, Comparatively To The T1-Non-Affected Tissue"

8.1. Methods

We checked if, in our sample of patients, the mean distance of T1 lesions from ventricular CSF was significantly different from the mean distance of the rest of the non-T1 affected parenchyma. To assess the mean distance from CSF of the T1 lesional load for each patient we used the layered distance map (as described by Pardini M et al, 2016), each layer's region being valued with integer numbers from 1 to 12 (reflecting the voxel distance from the periventricular deep zone to the subcortical WM, with zero value for the intraventricular CSF and 13 value for the cortical GM); we coregistered the 12-white-matter-layer map to the normal MNI space[138-141] and then multiplied the binary T1 lesion maps with the layer map and averaged the corresponding values on the layer map to obtain a mean distance value for the distribution of the T1 affected tissue. We performed the same process for the T1-normally-appearing WM.

We then performed a paired samples T-test to check for differences between the mean distances from ventricles of the T1-affected and T1-normal tissue.
Finally, we performed an age-at-mri corrected general linear model test to search for differences between the mean distances from ventricles of the T1-affected and T1-normal tissue.

8.2. Results

Here (Table 6) we present the average distances (and their standard deviation) from ventricles of the T1-affected and T1-normal tissue (on a 1-to-12 based scale). On the right, we reported the correlation p value for the paired sample T-test* and for the age corrected general linear model** performed as described in the methods section.

While a significant difference (p=0.017) was found, between the distance of the T1-affected and the T1-normally appearing WM, in our sample of patients, with the paired sample T-test*, this significance did not survive when testing with age-corrected general linear model**.

Table 6

DISTANCE FROM VENTRICLES	T1-lesioned	5.371 / 12 ± 1.144 / 12	] p=0.017* and p=0.585**
	T1-lesion-free	5.135 / 12 ± 0.824 / 12	

Results of the average values (± standard deviation) of distance -in "twelfths"- from the ventricular surface of the "T1-affected" versus the "T1-spared" WM tissue. On the right we showed the significance of their comparison by means of paired sample T-test and the loss of statistical significance if tested by age-corrected general linear model test**.*

9 . Discussion

We noticed that the amount of orientation dispersion of the axons in a brain region, as estimated by the NODDI mathematical model, does not seem to influence the probability of development of a T1-visible WM lesion (also known as “black hole”), when considering the whole brain, in our sample of multiple sclerosis patients. Conversely, the amount of neurite density seems to have an impact on the multiple sclerosis lesion evolution to black hole.

A higher coherence and compactness of structure in the myelin-rich WM areas could constitute a facilitating factor for the auto-inflammatory immune process against myelin antigens.
It is interesting to see that this effect, which appears significant when considered the whole brain, looks to be particularly prominent in the “deep WM layer”, which is the furthest-from-CSF part of WM.

We also noted that in the subpial layer, the closest to superficial CSF, orientation dispersion index assumes a close-to-significant role in the lesion-to-black-hole degeneration process, possibly underlying a different interaction between inflammatory factors and tissue structure, at different WM deepness levels.

Further magnetic resonance imaging studies and ex vivo histological investigations could better explore the mechanisms of interaction between the distance from CSF and the microstructure of WM.

In perspective, it will be interesting to verify whether the “black hole lesions” show differences in size, number, characteristics relatively to their distance from CSF (i.e. the brain inner and outer surface).

Another pending project is to assess the volumetric proportion of T1-lesioned tissue versus T1-spared tissue, relatively to each WM deepness level.

Furthermore, the rescan of the previously cross-sectionally studied population is in progress, such as the repetition of the lesion FLAIR and T1 segmentation. The study of the NODDI properties of the regions affected by progression of the FLAIR lesion to T1 black hole could confirm if there is a microstructural predicting factor which could facilitate the process of lesion degeneration.

Finally, the NODDI parametric WM normal microstructural atlas maps could be employed to assess the mechanisms of WM injury in other demyelinating processes and in other diseases where the WM is prominently affected.

List of figures

List of tables

List of publications and lectures

Position Sense Deficits at the Lower Limbs in Early Multiple Sclerosis: Clinical and Neural Correlates.
Iandolo R, Bommarito G, Falcitano L, Schiavi S, Piaggio N, Mancardi GL, Casadio M, Inglese M.
Neurorehabil Neural Repair. 2020 Mar;34(3):260-270. doi: 10.1177/1545968320902126. Epub 2020 Feb 7. PMID: 32028846

Preserved brain functional plasticity after upper limb task-oriented rehabilitation in progressive multiple sclerosis.
Boffa G, Tacchino A, Sbragia E, Schiavi S, Droby A, Piaggio N, Bommarito G, Girardi G, Mancardi GL, Brichetto G, Inglese M.
Eur J Neurol. 2019 Aug 16. doi: 10.1111/ene.14059. [Epub ahead of print] PMID: 31419353

Exploring mania-associated white matter injury by comparison with multiple sclerosis: a diffusion tensor imaging study.
Piaggio N, Schiavi S, Martino M, Bommarito G, Inglese M, Magioncalda P.
Psychiatry Res Neuroimaging. 2018 Sep 22;281:78-84. doi: 10.1016/j.pscychresns.2018.09.005. [Epub ahead of print] PMID: 30268035

White matter microstructure alterations correlate with terminally differentiated CD8+ effector T cell depletion in the peripheral blood in mania: Combined DTI and immunological investigation in the different phases of bipolar disorder.
Magioncalda P, Martino M, Tardito S, Sterlini B, Conio B, Marozzi V, Adavastro G, Capobianco L, Russo D, Parodi A, Kalli F, Nasi G, Altosole T, Piaggio N, Northoff G, Fenoglio D, Inglese M, Filaci G, Amore M.
Brain Behav Immun. 2018 May 1. pii: S0889-1591(18)30169-7. doi: 10.1016/j.bbi.2018.04.017. [Epub ahead of print] PMID: 29723656

Cord cross-sectional area at foramen magnum as a correlate of disability in amyotrophic lateral sclerosis.
Piaggio N, Pardini M, Roccatagliata L, Scialò C, Cabona C, Bonzano L, Inglese M, Mancardi GL, Caponnetto C.
Eur Radiol Exp. 2018 Jun 22;2:13. doi: 10.1186/s41747-018-0045-6. eCollection 2018 Dec. PMID: 29984352

Cerebellum and neurodegenerative diseases: beyond conventional MRI
Mormina E, Petracca M, Bommarito G, Piaggio N, Cocozza S and Inglese M
World J Radiol. 2017 Oct 28; 9(10): 371–388.
Published online 2017 Oct 28. doi: 10.4329/wjr.v9.i10.371

An engineered glove allows a quantitative integrated assessment of motor and cognitive impairment in multiple sclerosis
Gallo E, Laroni A, Pardini M, Inglese M, Signori A, Piaggio N, Lapucci C, Filippi L, Sbragia E, Meli R, Bommarito G, Cellerino M, Uccelli A, Mancardi GL, Sormani MP.
Abstract submitted to the 7th Joint ECTRIMS - ACTRIMS Meeting taking place in Paris, France from 25 - 28 October 2017

Different cognitive and pathological substrata of positive and negative emotion recognition in subjects with multiple sclerosis
Pardini M, Meli R, Piaggio N, Lapucci C, Sbragia E, Filippi L, Laroni A, Uccelli A, Mancardi GL, Inglese M.
Abstract submitted to the 7th Joint ECTRIMS - ACTRIMS Meeting taking place in Paris, France from 25 - 28 October 2017

Contrasting variability patterns in the default mode and sensorimotor networks balance in bipolar depression and mania.
Martino M, Magioncalda P, Huang Z, Conio B, Piaggio N, Duncan NW, Rocchi G, Escelsior A, Marozzi V, Wolff A, Inglese M, Amore M, Northoff G.
*Proc Natl Acad Sci U S A. 2016 Apr 26;113(17):4824-9. doi: 10.1073/pnas.1517558113. Epub 2016 Apr 11.*PMID: 27071087

Patterns of microstructural white matter abnormalities and their impact on cognitive dysfunction in the various phases of type I bipolar disorder.
Magioncalda P, Martino M, Conio B, Piaggio N, Teodorescu R, Escelsior A, Marozzi V, Rocchi G, Roccatagliata L, Northoff G, Inglese M, Amore M.
J Affect Disord. 2016 Mar 15;193:39-50. doi: 10.1016/j.jad.2015.12.050. Epub 2015 Dec 30. PMID: 26766032

Functional connectivity and neuronal variability of resting state activity in bipolar disorder-reduction and decoupling in anterior cortical midline structures.
Magioncalda P, Martino M, Conio B, Escelsior A, Piaggio N, Presta A, Marozzi V, Rocchi G, Anastasio L, Vassallo L, Ferri F, Roccatagliata L, Pardini M, Northoff G, Amore M.
Hum Brain Mapp. 2015 Feb;36(2):666-82. doi: 10.1002/hbm.22655. Epub 2014 Oct 12. PMID: 25307723

Abnormal functional-structural cingulum connectivity in mania: combined functional magnetic resonance imaging-diffusion tensor imaging investigation in different phases of bipolar disorder.
Martino M, Magioncalda P, Saiote C, Conio B, Escelsior A, Rocchi G, Piaggio N, Marozzi V, Huang Z, Ferri F, Amore M, Inglese M, Northoff G.
Acta Psychiatr Scand. 2016 Jun 7. doi: 10.1111/acps.12596. [Epub ahead of print] PMID: 27273612

Other academic activities during the PhD Course

- Was speaker for 4 hours in a ECM course targeted to medical doctors, physiotherapists, and other rehabilitation professionals, titled: „Ricerca nella Sclerosi Multipla: Le Tecnologie al Servizio della Riabilitazione“, 2 and 3 december 2017

- Was the supervisor of 3 medical students for the preparation of their thesis, titled :

> « Atrofia Cerebrale in Sclerosi Multipla. Confronto del parametro di NeuroRM Brain Parenchymal Fraction in sequenze 3D-FSPGR e 3D-FLAIR, con procedura totalmente automatizzata », july 2017.
>
> « Area Spinale Cervicale a livello del Forame Magno e Disabilità nella Sclerosi Laterale Amiotrofica: uno Studio Pilota », july 2017.
>
> « Ottimizzazione del processo di calcolo del carico lesionale in Sclerosi Multipla: confronto tra segmentazione manuale e alcuni algoritmi automatizzati sia con sequenze di risonanza magnetica 3D FLAIR, che con tecnica FLAIR2 », march 2018.

References

1. Bloch, F., *Nuclear induction.* Physical review, 1946. 70(7-8): p. 460.
2. Purcell, E.M., H.C. Torrey, and R.V. Pound, *Resonance absorption by nuclear magnetic moments in a solid.* Physical review, 1946. 69(1-2): p. 37.
3. Hawkes, R., et al., *Nuclear magnetic resonance (NMR) tomography of the brain: a preliminary clinical assessment with demonstration of pathology.* Journal of Computer Assisted Tomography, 1980. 4(5): p. 577-586.
4. Jones, D.K., *Diffusion mri*. 2010: Oxford University Press.
5. Chilla, G.S., et al., *Diffusion weighted magnetic resonance imaging and its recent trend-a survey.* Quant Imaging Med Surg, 2015. 5(3): p. 407-22.
6. Pasternak, O., et al., *Advances in microstructural diffusion neuroimaging for psychiatric disorders.* Neuroimage, 2018. 182: p. 259-282.
7. Zhang, H., et al., *NODDI: practical in vivo neurite orientation dispersion and density imaging of the human brain.* Neuroimage, 2012. 61(4): p. 1000-1016.
8. Rae, C.L., et al., *Deficits in neurite density underlie white matter structure abnormalities in first-episode psychosis.* Biological psychiatry, 2017. 82(10): p. 716-725.
9. Nazeri, A., et al., *Gray matter neuritic microstructure deficits in schizophrenia and bipolar disorder.* Biological psychiatry, 2017. 82(10): p. 726-736.
10. Van Essen, D.C., et al., *The Human Connectome Project: a data acquisition perspective.* Neuroimage, 2012. 62(4): p. 2222-2231.
11. G.Sery, P., *Ubuntu Linux For Dummies*. Vol. Chapter 1. 2007: John Wiley & Sons.
12. Bellis, M. *The Unusual History of Microsoft Windows*. 2020 13-11-2020]; Available from: thoughtco.com/unusual-history-of-microsoft-windows-1992140.
13. GNU-Project. *BASH Readme File*. 2014 13-11-2020]; Available from: https://www.gnu.org/software/bash/.
14. Jenkinson, M., et al., *FSL.* Neuroimage, 2012. 62(2): p. 782-90.
15. Sobie, E.A., *An introduction to MATLAB.* Sci Signal, 2011. 4(191): p. tr7.
16. Zhang, H., et al., *NODDI: practical in vivo neurite orientation dispersion and density imaging of the human brain.* Neuroimage, 2012. 61(4): p. 1000-16.
17. Zhang, H., et al. *NODDI Matlab Toolbox, Official Webpage*. 2020 15-11-2020]; Available from: http://mig.cs.ucl.ac.uk/index.php?n=Tutorial.NODDImatlab.

18. International.Business.Machines.Corporation. *SPSS official page*. 1968 30-11-2020]; Available from: https://www.ibm.com/analytics/spss-statistics-software.
19. Lublin, F.D., et al., *Defining the clinical course of multiple sclerosis: the 2013 revisions.* Neurology, 2014. 83(3): p. 278-86.
20. Reich, D.S., C.F. Lucchinetti, and P.A. Calabresi, *Multiple Sclerosis.* N Engl J Med, 2018. 378(2): p. 169-180.
21. G.B.D.Multiple.Sclerosis.Collaborators, *Global, regional, and national burden of multiple sclerosis 1990-2016: a systematic analysis for the Global Burden of Disease Study 2016.* Lancet Neurol, 2019. 18(3): p. 269-285.
22. Browne, P., et al., *Atlas of Multiple Sclerosis 2013: A growing global problem with widespread inequity.* Neurology, 2014. 83(11): p. 1022-4.
23. Koch-Henriksen, N. and P.S. Sorensen, *The changing demographic pattern of multiple sclerosis epidemiology.* Lancet Neurol, 2010. 9(5): p. 520-32.
24. Orton, S.M., et al., *Sex ratio of multiple sclerosis in Canada: a longitudinal study.* Lancet Neurol, 2006. 5(11): p. 932-6.
25. Kingwell, E., et al., *Relative mortality and survival in multiple sclerosis: findings from British Columbia, Canada.* J Neurol Neurosurg Psychiatry, 2012. 83(1): p. 61-6.
26. Leray, E., et al., *Excess Mortality in Patients with Multiple Sclerosis Starts at 20 Years from Clinical Onset: Data from a Large-Scale French Observational Study.* PLoS One, 2015. 10(7): p. e0132033.
27. Belbasis, L., et al., *Environmental factors and risk of multiple sclerosis: Findings from meta-analyses and Mendelian randomization studies.* Mult Scler, 2020. 26(4): p. 397-404.
28. Belbasis, L., et al., *Environmental risk factors and multiple sclerosis: an umbrella review of systematic reviews and meta-analyses.* Lancet Neurol, 2015. 14(3): p. 263-73.
29. Dendrou, C.A., L. Fugger, and M.A. Friese, *Immunopathology of multiple sclerosis.* Nat Rev Immunol, 2015. 15(9): p. 545-58.
30. Ebers, G.C., et al., *A population-based study of multiple sclerosis in twins.* N Engl J Med, 1986. 315(26): p. 1638-42.
31. Hollenbach, J.A. and J.R. Oksenberg, *The immunogenetics of multiple sclerosis: A comprehensive review.* J Autoimmun, 2015. 64: p. 13-25.
32. Koch, M.W., et al., *Global transcriptome profiling of mild relapsing-remitting versus primary progressive multiple sclerosis.* Eur J Neurol, 2018. 25(4): p. 651-658.
33. Lassmann, H., *Pathogenic Mechanisms Associated With Different Clinical Courses of Multiple Sclerosis.* Front Immunol, 2018. 9: p. 3116.
34. Trapp, B.D. and K.A. Nave, *Multiple sclerosis: an immune or neurodegenerative disorder?* Annu Rev Neurosci, 2008. 31: p. 247-69.
35. Stys, P.K., et al., *Will the real multiple sclerosis please stand up?* Nat Rev Neurosci, 2012. 13(7): p. 507-14.

36. Miller, D.H., D.T. Chard, and O. Ciccarelli, *Clinically isolated syndromes.* Lancet Neurol, 2012. 11(2): p. 157-69.
37. Thompson, A.J., et al., *Diagnosis of multiple sclerosis: 2017 revisions of the McDonald criteria.* Lancet Neurol, 2018. 17(2): p. 162-173.
38. Lapucci, C., et al., *How much do periventricular lesions assist in distinguishing migraine with aura from CIS?* Neurology, 2019. 92(15): p. e1739-e1744.
39. Sati, P., et al., *The central vein sign and its clinical evaluation for the diagnosis of multiple sclerosis: a consensus statement from the North American Imaging in Multiple Sclerosis Cooperative.* Nat Rev Neurol, 2016. 12(12): p. 714-722.
40. Brownlee, W.J., *Do spinal cord lesions matter in patients with clinically isolated syndrome and early MS?* Mult Scler, 2018. 24(4): p. 430-431.
41. Wattjes, M.P., et al., *Evidence-based guidelines: MAGNIMS consensus guidelines on the use of MRI in multiple sclerosis--establishing disease prognosis and monitoring patients.* Nat Rev Neurol, 2015. 11(10): p. 597-606.
42. Rovira, A., et al., *Evidence-based guidelines: MAGNIMS consensus guidelines on the use of MRI in multiple sclerosis-clinical implementation in the diagnostic process.* Nat Rev Neurol, 2015. 11(8): p. 471-82.
43. Eshaghi, A., et al., *Deep gray matter volume loss drives disability worsening in multiple sclerosis.* Ann Neurol, 2018. 83(2): p. 210-222.
44. Durand-Dubief, F., et al., *Reliability of longitudinal brain volume loss measurements between 2 sites in patients with multiple sclerosis: comparison of 7 quantification techniques.* AJNR Am J Neuroradiol, 2012. 33(10): p. 1918-24.
45. Roosendaal, S.D., et al., *Resting state networks change in clinically isolated syndrome.* Brain, 2010. 133(Pt 6): p. 1612-21.
46. Koubiyr, I., et al., *Dynamic modular-level alterations of structural-functional coupling in clinically isolated syndrome.* Brain, 2019. 142(11): p. 3428-3439.
47. Liu, Y., et al., *Disrupted Module Efficiency of Structural and Functional Brain Connectomes in Clinically Isolated Syndrome and Multiple Sclerosis.* Front Hum Neurosci, 2018. 12: p. 138.
48. Shu, N., et al., *Disrupted topological organization of structural and functional brain connectomes in clinically isolated syndrome and multiple sclerosis.* Sci Rep, 2016. 6: p. 29383.
49. Shu, N., et al., *Progressive brain rich-club network disruption from clinically isolated syndrome towards multiple sclerosis.* Neuroimage Clin, 2018. 19: p. 232-239.
50. Patel, K.R., et al., *Structural disconnection is responsible for increased functional connectivity in multiple sclerosis.* Brain Struct Funct, 2018. 223(5): p. 2519-2526.
51. Hawellek, D.J., et al., *Increased functional connectivity indicates the severity of cognitive impairment in multiple sclerosis.* Proc Natl Acad Sci U S A, 2011. 108(47): p. 19066-71.

52. Tewarie, P., et al., *Explaining the heterogeneity of functional connectivity findings in multiple sclerosis: An empirically informed modeling study.* Hum Brain Mapp, 2018. 39(6): p. 2541-2548.
53. Pinter, D., et al., *Morphological MRI phenotypes of multiple sclerosis differ in resting-state brain function.* Sci Rep, 2019. 9(1): p. 16221.
54. Rocca, M.A., et al., *Large-scale neuronal network dysfunction in relapsing-remitting multiple sclerosis.* Neurology, 2012. 79(14): p. 1449-57.
55. Tommasin, S., et al., *Relation between functional connectivity and disability in multiple sclerosis: a non-linear model.* J Neurol, 2018. 265(12): p. 2881-2892.
56. Cercignani, M. and C. Gandini Wheeler-Kingshott, *From micro- to macro-structures in multiple sclerosis: what is the added value of diffusion imaging.* NMR in Biomedicine, 2019. 32(4): p. e3888.
57. Filippi, M., et al., *A quantitative study of water diffusion in multiple sclerosis lesions and normal-appearing white matter using echo-planar imaging.* Archives of neurology, 2000. 57(7): p. 1017-1021.
58. Werring, D., et al., *Diffusion tensor imaging of lesions and normal-appearing white matter in multiple sclerosis.* Neurology, 1999. 52(8): p. 1626-1626.
59. Ciccarelli, O., et al., *Investigation of MS normal-appearing brain using diffusion tensor MRI with clinical correlations.* Neurology, 2001. 56(7): p. 926-933.
60. Cavallari, M., et al., *Microstructural changes in the striatum and their impact on motor and neuropsychological performance in patients with multiple sclerosis.* PloS one, 2014. 9(7): p. e101199.
61. Hannoun, S., et al., *Diffusion tensor–MRI evidence for extra-axonal neuronal degeneration in caudate and thalamic nuclei of patients with multiple sclerosis.* American Journal of Neuroradiology, 2012. 33(7): p. 1363-1368.
62. Calabrese, M., et al., *Cortical diffusion-tensor imaging abnormalities in multiple sclerosis: a 3-year longitudinal study.* Radiology, 2011. 261(3): p. 891-898.
63. Beaulieu, C., *Diffusion MRI: from quantitative measurement to in vivo neuroanatomy (Johansen-Berg H, Behrens TEJ, eds)*. 2009, London: Elsevier.
64. Klawiter, E.C., et al., *Radial diffusivity predicts demyelination in ex vivo multiple sclerosis spinal cords.* Neuroimage, 2011. 55(4): p. 1454-1460.
65. Song, S.-K., et al., *Demyelination increases radial diffusivity in corpus callosum of mouse brain.* Neuroimage, 2005. 26(1): p. 132-140.
66. Cercignani, M., *About" axial" and" radial" diffusivities.* Magnetic resonance in medicine: official journal of the Society of Magnetic Resonance in Medicine/Society of Magnetic Resonance in Medicine, 2009. 61(5): p. 1255-1260.
67. Wheeler-Kingshott, C.A., et al., *A new approach to structural integrity assessment based on axial and radial diffusivities.* Functional neurology, 2012. 27(2): p. 85.

68. Stejskal, E.O. and J.E. Tanner, *Spin diffusion measurements: spin echoes in the presence of a time-dependent field gradient.* The journal of chemical physics, 1965. 42(1): p. 288-292.
69. Ong, H.H., et al., *Indirect measurement of regional axon diameter in excised mouse spinal cord with q-space imaging: simulation and experimental studies.* Neuroimage, 2008. 40(4): p. 1619-1632.
70. Fujiyoshi, K., et al., *Application of q-space diffusion MRI for the visualization of white matter.* Journal of Neuroscience, 2016. 36(9): p. 2796-2808.
71. Assaf, Y., A. Mayk, and Y. Cohen, *Displacement imaging of spinal cord using q-space diffusion-weighted MRI.* Magnetic Resonance in Medicine: An Official Journal of the International Society for Magnetic Resonance in Medicine, 2000. 44(5): p. 713-722.
72. Nossin-Manor, R., R. Duvdevani, and Y. Cohen, *q-Space high b value diffusion MRI of hemi-crush in rat spinal cord: evidence for spontaneous regeneration.* Magnetic resonance imaging, 2002. 20(3): p. 231-241.
73. Steinman, L., *Assessment of animal models for MS and demyelinating disease in the design of rational therapy.* Neuron, 1999. 24(3): p. 511-514.
74. Biton, I.E., et al., *Improved detectability of experimental allergic encephalomyelitis in excised swine spinal cords by high b-value q-space DWI.* Experimental neurology, 2005. 195(2): p. 437-446.
75. Assaf, Y., et al., *High b-value q-space analyzed diffusion-weighted MRI: application to multiple sclerosis.* Magnetic Resonance in Medicine: An Official Journal of the International Society for Magnetic Resonance in Medicine, 2002. 47(1): p. 115-126.
76. Assaf, Y., et al., *White matter changes in multiple sclerosis: correlation of q-space diffusion MRI and 1H MRS.* Magnetic resonance imaging, 2005. 23(6): p. 703-710.
77. Farrell, J.A., et al., *High b-value q-space diffusion-weighted MRI of the human cervical spinal cord in vivo: feasibility and application to multiple sclerosis.* Magnetic Resonance in Medicine: An Official Journal of the International Society for Magnetic Resonance in Medicine, 2008. 59(5): p. 1079-1089.
78. Abdel-Aziz, K., et al., *Evidence for early neurodegeneration in the cervical cord of patients with primary progressive multiple sclerosis.* Brain, 2015. 138(6): p. 1568-1582.
79. Tanikawa, M., et al., *q-Space Myelin Map imaging for longitudinal analysis of demyelination and remyelination in multiple sclerosis patients treated with fingolimod: A preliminary study.* Journal of the neurological sciences, 2017. 373: p. 352-357.
80. de Kouchkovsky, I., et al., *Quantification of normal-appearing white matter tract integrity in multiple sclerosis: a diffusion kurtosis imaging study.* Journal of neurology, 2016. 263(6): p. 1146-1155.
81. Yoshida, M., et al., *Diffusional kurtosis imaging of normal-appearing white matter in multiple sclerosis: preliminary clinical experience.* Japanese journal of radiology, 2013. 31(1): p. 50-55.

82. Qian, W., et al., *Application of diffusional kurtosis imaging to detect occult brain damage in multiple sclerosis and neuromyelitis optica.* NMR in Biomedicine, 2016. 29(11): p. 1536-1545.
83. Takemura, M.Y., et al., *Alterations of the optic pathway between unilateral and bilateral optic nerve damage in multiple sclerosis as revealed by the combined use of advanced diffusion kurtosis imaging and visual evoked potentials.* Magnetic resonance imaging, 2017. 39: p. 24-30.
84. Wang, Y., et al., *Quantification of increased cellularity during inflammatory demyelination.* Brain, 2011. 134(12): p. 3590-3601.
85. Wang, Y., et al., *Differentiation and quantification of inflammation, demyelination and axon injury or loss in multiple sclerosis.* Brain, 2015. 138(5): p. 1223-1238.
86. Barkhof, F., *The clinico-radiological paradox in multiple sclerosis revisited.* Current opinion in neurology, 2002. 15(3): p. 239-245.
87. Bergsland, N., et al., *Corticospinal tract integrity is related to primary motor cortex thinning in relapsing–remitting multiple sclerosis.* Multiple Sclerosis Journal, 2015. 21(14): p. 1771-1780.
88. Hubbard, E.A., et al., *Diffusion tensor imaging of the corticospinal tract and walking performance in multiple sclerosis.* Journal of the neurological sciences, 2016. 363: p. 225-231.
89. Lin, X., et al., *'Importance sampling'in MS: use of diffusion tensor tractography to quantify pathology related to specific impairment.* Journal of the neurological sciences, 2005. 237(1-2): p. 13-19.
90. Gorgoraptis, N., et al., *Combining tractography and cortical measures to test system-specific hypotheses in multiple sclerosis.* Multiple Sclerosis Journal, 2010. 16(5): p. 555-565.
91. Dousset, V., et al., *Experimental allergic encephalomyelitis and multiple sclerosis: lesion characterization with magnetization transfer imaging.* Radiology, 1992. 182(2): p. 483-491.
92. Pardini, M., et al., *Motor network efficiency and disability in multiple sclerosis.* Neurology, 2015. 85(13): p. 1115-1122.
93. Dousset, V., *Magnetization transfer imaging in vivo study of normal brain tissues and characterization of multiple sclerosis and experimental allergic encephalomyelitis lesions.* Journal of neuroradiology= Journal de neuroradiologie, 1993. 20(4): p. 297.
94. Koenig, K.A., et al., *The relationship between cognitive function and high-resolution diffusion tensor MRI of the cingulum bundle in multiple sclerosis.* Multiple Sclerosis Journal, 2015. 21(14): p. 1794-1801.
95. Pardini, M., et al., *Cingulum bundle alterations underlie subjective fatigue in multiple sclerosis.* Multiple Sclerosis Journal, 2015. 21(4): p. 442-447.
96. Johansen-Berg, H. and T.E. Behrens, *Just pretty pictures? What diffusion tractography can add in clinical neuroscience.* Current opinion in neurology, 2006. 19(4): p. 379.

97. Sporns, O., G. Tononi, and R. Kötter, *The human connectome: a structural description of the human brain.* PLoS Comput Biol, 2005. 1(4): p. e42.
98. de Reus, M.A. and M.P. Van den Heuvel, *The parcellation-based connectome: limitations and extensions.* Neuroimage, 2013. 80: p. 397-404.
99. Papathanassiou, T.-M.N.L.B. and D.C.F.E.O. Delcroix, *anatomical labeling of activations in SPM using a macroscopic anatomical parcellation of the MNI MRI single-subject brain.* Neuroimage, 2002. 15: p. 273-289.
100. Scholtens, L.H., et al., *An mri von economo–koskinas atlas.* NeuroImage, 2018. 170: p. 249-256.
101. Hagmann, P., et al., *Mapping the structural core of human cerebral cortex.* PLoS Biol, 2008. 6(7): p. e159.
102. Craddock, R.C., et al., *A whole brain fMRI atlas generated via spatially constrained spectral clustering.* Human brain mapping, 2012. 33(8): p. 1914-1928.
103. Bonavita, S., et al., *Computer-aided cognitive rehabilitation improves cognitive performances and induces brain functional connectivity changes in relapsing remitting multiple sclerosis patients: an exploratory study.* Journal of neurology, 2015. 262(1): p. 91-100.
104. Campbell, J., et al., *A randomised controlled trial of efficacy of cognitive rehabilitation in multiple sclerosis: a cognitive, behavioural, and MRI study.* Neural plasticity, 2016. 2016.
105. van den Heuvel, M.P., et al., *Abnormal rich club organization and functional brain dynamics in schizophrenia.* JAMA psychiatry, 2013. 70(8): p. 783-792.
106. van den Heuvel, M.P., et al., *Aberrant frontal and temporal complex network structure in schizophrenia: a graph theoretical analysis.* Journal of Neuroscience, 2010. 30(47): p. 15915-15926.
107. Lemkaddem, A., et al., *Connectivity and tissue microstructural alterations in right and left temporal lobe epilepsy revealed by diffusion spectrum imaging.* NeuroImage: Clinical, 2014. 5: p. 349-358.
108. Romascano, D., et al., *Multicontrast connectometry: A new tool to assess cerebellum alterations in early relapsing-remitting multiple sclerosis.* Human brain mapping, 2015. 36(4): p. 1609-1619.
109. Shu, N., et al., *Disrupted topological organization of structural and functional brain connectomes in clinically isolated syndrome and multiple sclerosis.* Scientific reports, 2016. 6(1): p. 1-11.
110. Gili, T., et al., *Regional brain atrophy and functional disconnection across Alzheimer's disease evolution.* Journal of Neurology, Neurosurgery & Psychiatry, 2011. 82(1): p. 58-66.
111. Palesi, F., et al., *Exploring patterns of alteration in Alzheimer's disease brain networks: a combined structural and functional connectomics analysis.* Frontiers in neuroscience, 2016. 10: p. 380.

112. Shu, N., et al., *Diffusion tensor tractography reveals disrupted topological efficiency in white matter structural networks in multiple sclerosis.* Cerebral cortex, 2011. 21(11): p. 2565-2577.
113. Aerts, H., et al., *Brain networks under attack: robustness properties and the impact of lesions.* Brain, 2016. 139(12): p. 3063-3083.
114. Fornito, A., *Graph theoretic analysis of human brain networks*, in *FMRI techniques and protocols*. 2016, Springer. p. 283-314.
115. Zubizarreta, I., et al. *The Sys4MS project: personalizing health care in multiple sclerosis using systems medicine tools*. in *Multiple Sclerosis Journal*. 2018. Sage Publications Ltd 1 Olivers Yard, 55 City Road, London Ec1y 1sp, England.
116. Glasser, M.F., et al., *The human connectome project's neuroimaging approach.* Nature neuroscience, 2016. 19(9): p. 1175-1187.
117. Toga, A.W., et al., *Mapping the human connectome.* Neurosurgery, 2012. 71(1): p. 1-5.
118. USC, *The Human Connectome Project Data Archive.* 2018.
119. GadElkarim, J.J., et al. *TDF-Tract: probabilistic tractography using the tensor distribution function*. in *2011 IEEE International Symposium on Biomedical Imaging: From Nano to Macro*. 2011. IEEE.
120. Noseworthy, J.H., *Progress in determining the causes and treatment of multiple sclerosis.* Nature, 1999. 399(6738): p. A40-A47.
121. Haider, L., et al., *The topograpy of demyelination and neurodegeneration in the multiple sclerosis brain.* Brain, 2016. 139(3): p. 807-815.
122. Mainero, C., et al., *A gradient in cortical pathology in multiple sclerosis by in vivo quantitative 7 T imaging.* Brain, 2015. 138(4): p. 932-945.
123. Adams, C., et al., *Periventricular lesions in multiple sclerosis: their perivenous origin and relationship to granular ependymitis.* Neuropathology and applied neurobiology, 1987. 13(2): p. 141-152.
124. Bö, L., et al., *Grey matter pathology in multiple sclerosis.* Acta Neurologica Scandinavica, 2006. 113: p. 48-50.
125. Lassmann, H., *Multiple sclerosis: lessons from molecular neuropathology.* Experimental neurology, 2014. 262: p. 2-7.
126. Pardini, M., et al., *Relationship of grey and white matter abnormalities with distance from the surface of the brain in multiple sclerosis.* Journal of Neurology, Neurosurgery & Psychiatry, 2016. 87(11): p. 1212-1217.
127. Pardini, M., et al., *The relationship between cortical lesions and periventricular NAWM abnormalities suggests a shared mechanism of injury in primary-progressive MS.* NeuroImage: Clinical, 2017. 16: p. 111-115.
128. Tóth, E., et al., *Gray matter atrophy is primarily related to demyelination of lesions in multiple sclerosis: a diffusion tensor imaging MRI study.* Frontiers in neuroanatomy, 2017. 11: p. 23.
129. Brown, J.W.L., et al., *An abnormal periventricular magnetization transfer ratio gradient occurs early in multiple sclerosis.* Brain, 2017. 140(2): p. 387-398.

130. Schneider, T., et al., *Sensitivity of multi-shell NODDI to multiple sclerosis white matter changes: a pilot study.* Functional neurology, 2017. 32(2): p. 97.
131. Valla, R., *Simulations Of Synthetic Diffusion Mri Data Based On Brownian Motion.*
132. Hall, M.G. and D.C. Alexander, *Convergence and parameter choice for Monte-Carlo simulations of diffusion MRI.* IEEE transactions on medical imaging, 2009. 28(9): p. 1354-1364.
133. Alexander, D.C., et al., *Orientationally invariant indices of axon diameter and density from diffusion MRI.* Neuroimage, 2010. 52(4): p. 1374-1389.
134. Panagiotaki, E., et al. *High-fidelity meshes from tissue samples for diffusion MRI simulations*. in *International Conference on Medical Image Computing and Computer-Assisted Intervention*. 2010. Springer.
135. Siow, B., et al., *Estimation of pore size in a microstructure phantom using the optimised gradient waveform diffusion weighted NMR sequence.* Journal of Magnetic Resonance, 2012. 214: p. 51-60.
136. Richardson, S., et al., *A viable isolated tissue system: a tool for detailed MR measurements and controlled perturbation in physiologically stable tissue.* Magnetic Resonance in Medicine, 2013. 69(6): p. 1603-1610.
137. Sato, K., et al., *Understanding microstructure of the brain by comparison of neurite orientation dispersion and density imaging (NODDI) with transparent mouse brain.* Acta radiologica open, 2017. 6(4): p. 2058460117703816.
138. Montreal.Neurological.Institute, *ICBM 152 Nonlinear Atlases Version 2009.* 2009.
139. Collins, D.L., et al. *ANIMAL+ INSECT: improved cortical structure segmentation*. in *Biennial International Conference on Information Processing in Medical Imaging*. 1999. Springer.
140. Fonov, V., et al., *Unbiased average age-appropriate atlases for pediatric studies.* Neuroimage, 2011. 54(1): p. 313-327.
141. Fonov, V.S., et al., *Unbiased nonlinear average age-appropriate brain templates from birth to adulthood.* NeuroImage, 2009(47): p. S102.